
Robustness Disparities in Commercial Face Detection

Samuel Dooley
University of Maryland
sdooley1@cs.umd.edu

Tom Goldstein
University of Maryland
tomg@cs.umd.edu

John P. Dickerson
University of Maryland
john@cs.umd.edu

Abstract

Facial detection and analysis systems have been deployed by large companies and critiqued by scholars and activists for the past decade. Critiques that focus on system performance analyze disparity of the system’s output, i.e., how frequently is a face detected for different Fitzpatrick skin types or perceived genders. However, we focus on the robustness of these system outputs under noisy natural perturbations. We present the first of its kind detailed benchmark of the robustness of three such systems: Amazon Rekognition, Microsoft Azure, and Google Cloud Platform. We use both standard and recently released academic facial datasets to quantitatively analyze trends in robustness for each. Across all the datasets and systems, we generally find that photos of individuals who are *older*, *masculine presenting*, of *darker skin type*, or have *dim lighting* are more susceptible to errors than their counterparts in other identities.

1 Introduction

Face detection systems identify the presence and location of faces in images and video. Automated face detection is a core component of myriad systems—including *face recognition technologies* (FRT), wherein a detected face is matched against a database of faces, typically for identification or verification purposes. FRT-based systems are widely deployed [Hartzog, 2020, Derringer, 2019, Weise and Singer, 2020]. Automated face recognition enables capabilities ranging from the relatively morally neutral (e.g., searching for photos on a personal phone [Google, 2021]) to morally laden (e.g., widespread citizen surveillance [Hartzog, 2020], or target identification in warzones [Marson and Forrest, 2021]). Legal and social norms regarding the usage of FRT are evolving [e.g., Grother et al., 2019]. For example, in June 2021, the first county-wide ban on its use for policing [see, e.g., Garvie, 2016] went into effect in the US [Gutman, 2021]. Some use cases for FRT will be deemed socially repugnant and thus be either legally or *de facto* banned from use; yet, it is likely that pervasive use of facial analysis will remain—albeit with more guardrails than are found today [Singer, 2018].

One such guardrail that has spurred positive, though insufficient, improvements and widespread attention is the use of benchmarks. For example, in late 2019, the US National Institute of Standards and Technology (NIST) adapted its venerable Face Recognition Vendor Test (FRVT) to explicitly include concerns for demographic effects [Grother et al., 2019], ensuring such concerns propagate into industry systems. Yet, differential treatment by FRT of groups has been known for at least a decade [e.g., Klare et al., 2012, El Khiyari and Wechsler, 2016], and more recent work spearheaded by Buolamwini and Gebru [2018] uncovers unequal performance at the phenotypic subgroup level. That latter work brought widespread public, and thus burgeoning regulatory, attention to bias in FRT [e.g., Lohr, 2018, Kantayya, 2020].

One yet unexplored benchmark examines the bias present in a system’s robustness (e.g., to noise, or to different lighting conditions), both in aggregate and with respect to different dimensions of the population on which it will be used. Many detection and recognition systems are not built in house, instead making use of commercial cloud-based “ML as a Service” (MLaaS) platforms offered by tech giants such as Amazon, Microsoft, Google, Megvii, etc. The implementation details of those

systems are not exposed to the end user—and even if they were, quantifying their failure modes would be difficult. With this in mind, our **main contribution** is a wide *robustness benchmark* of three commercial-grade face detection systems (accessed via Amazon’s Rekognition, Microsoft’s Azure, and Google Cloud Platform’s face detection APIs). For fifteen types of realistic noise, and five levels of severity per type of noise [Hendrycks and Dietterich, 2019], we test both APIs against images in each of four well-known datasets. Across these more than 5,000,000 noisy images, we analyze the impact of noise on face detection performance. Perhaps unsurprisingly, we find that noise decreases overall performance, though the result from our study confirms the previous findings of Hendrycks and Dietterich [2019]. Further, different types of noise impact, in an unbiased way, cross sections of the population of images (e.g., based on Fitzgerald skin type, age, self-identified gender, and intersections of those dimensions). Our method is extensible and can be used to quantify the robustness of other detection and FRT systems, and adds to the burgeoning literature supporting the necessity of explicitly considering bias in ML systems with morally-laden downstream uses.

2 Related Work

We briefly overview additional related work in the two core areas addressed by our benchmark: robustness to noise and demographic disparity in facial detection and recognition. That latter point overlaps heavily with the fairness in machine learning literature; for additional coverage of that broader ecosystem and discussion around bias in machine learning writ large, we direct the reader to survey works due to Chouldechova and Roth [2018] and Barocas et al. [2019].

Demographic effects in facial detection and recognition. The existence of differential performance of facial detection and recognition on groups and subgroups of populations has been explored in a variety of settings. Earlier work [e.g., Klare et al., 2012, O’Toole et al., 2012] focuses on single-demographic effects (specifically, race and gender) in pre-deep-learning face detection and recognition. Buolamwini and Gebre [2018] uncovers unequal performance at the phenotypic subgroup level in, specifically, a gender classification task powered by commercial systems. That work, typically referred to as “Gender Shades,” has been and continues to be hugely impactful both within academia and at the industry level. Indeed, Raji and Buolamwini [2019] provide a follow-on analysis, exploring the impact of the Buolamwini and Gebre [2018] paper publicly disclosing performance results, for specific systems, with respect to demographic effects; they find that their named companies (IBM, Microsoft, and Megvii) updated their APIs within a year to address some concerns that were surfaced. Subsequently, the late 2019 update to the NIST FRVT provides evidence that commercial platforms are continuing to focus on performance at the group and subgroup level [Grother et al., 2019]. Further recent work explores these demographic questions with a focus on Indian election candidates [Jain and Parsheera, 2021]. We see our benchmark as adding to this literature by, for the first time, addressing both noise and demographic effects on commercial platforms’ face detection offerings.

In this work, we focus on *measuring* the impact of noise on a classification task, like that of Wilber et al. [2016]; indeed, a core focus of our benchmark is to *quantify* relative drops in performance conditioned on an input datapoint’s membership in a particular group. We view our work as a *benchmark*, that is, it focuses on quantifying and measuring, decidedly not providing a new method to “fix” or otherwise mitigate issues of demographic inequity in a system. Toward that latter point, existing work on “fixing” unfair systems can be split into three (or, arguably, four [Savani et al., 2020]) focus areas: pre-, in-, and post-processing. Pre-processing work largely focuses on dataset curation and preprocessing [e.g., Feldman et al., 2015, Ryu et al., 2018, Quadrianto et al., 2019, Wang and Deng, 2020]. In-processing often constrains the ML training method or optimization algorithm itself [e.g., Zafar et al., 2017b,a, 2019, Donini et al., 2018, Goel et al., 2018, Padala and Gujar, 2020, Agarwal et al., 2018, Wang and Deng, 2020, Martinez et al., 2020, Diana et al., 2020, Lahoti et al., 2020], or focuses explicitly on so-called fair representation learning [e.g., Adeli et al., 2021, Dwork et al., 2012, Zemel et al., 2013, Edwards and Storkey, 2016, Madras et al., 2018, Beutel et al., 2017, Wang et al., 2019]. Post-processing techniques adjust decisioning at inference time to align with quantitative fairness definitions [e.g., Hardt et al., 2016, Wang et al., 2020].

Robustness to noise. Quantifying, and improving, the robustness to noise of face detection and recognition systems is a decades-old research challenge. Indeed, mature challenges like NIST’s Facial Recognition Vendor Test (FRVT) have tested for robustness since the early 2000s [Phillips et al., 2007]. We direct the reader to a comprehensive introduction to an earlier robustness challenge



Figure 1: Our benchmark consists of 5,066,312 images of the 15 types of algorithmically generated corruptions produced by ImageNet-C. We use data from four datasets (Adience, CCD, MIAP, and UTKFace) and present examples of corruptions from each dataset here.

due to NIST [Phillips et al., 2011]; that work describes many of the specific challenges faced by face detection and recognition systems, often grouped into Pose, Illumination, and Expression (PIE). It is known that commercial systems still suffer from degradation due to noise [e.g., Hosseini et al., 2017]; none of this work also addresses the intersection of noise with bias, as we do. Recently, *adversarial* attacks have been proposed that successfully break commercial face recognition systems [Shan et al., 2020, Cherepanova et al., 2021]; we note that our focus is on *natural* noise, as motivated by Hendrycks and Dietterich [2019] by their ImageNet-C benchmark. Literature at the intersection of adversarial robustness and fairness is nascent and does not address commercial platforms [e.g., Singh et al., 2020, Nanda et al., 2021]. To our knowledge, our work is the first systematic benchmark for commercial face detection systems that addresses, comprehensively, noise and its differential impact on (sub)groups of the population.

3 Experimental Description

Datasets and Protocol. This benchmark uses four datasets to evaluate the robustness of Amazon AWS and Microsoft Azure’s face detection systems. They are described below and a repository for the experiments can be found here: <https://github.com/dooleys/Robustness-Disparities-in-Commercial-Face-Detection>.

The Open Images Dataset V6 – Extended; More Inclusive Annotations for People (**MIAP**) dataset [Schumann et al., 2021] was released by Google in May 2021 as an extension of the popular, permissive-licensed Open Images Dataset specifically designed to improve annotations of humans. For each image, every human is exhaustively annotated with bounding boxes for the entirety of their person visible in the image. Each annotation also has perceived gender (Feminine/Masculine/Unknown) presentation and perceived age (Young, Middle, Old, Unknown) presentation.

The Casual Conversations Dataset (**CCD**) [Hazirbas et al., 2021] was released by Facebook in April 2021 under limited license and includes videos of actors. Each actor consented to participate in an ML dataset and provided their self-identification of age and gender (coded as Female, Male, and Other), each actor’s skin type was rated on the Fitzpatrick scale [Fitzpatrick, 1988], and each video was rated for its ambient light quality. For our benchmark, we extracted one frame from each video.

The **Adience** dataset [Eidinger et al., 2014] under a CC license, includes cropped images of faces from images “in the wild”. Each cropped image contains only one primary, centered face, and each face is annotated by an external evaluator for age and gender (Female/Male). The ages are reported as member of 8 age range buckets: 0-2; 3-7; 8-14; 15-24; 25-35; 36-45; 46-59; 60+.

Finally, the **UTKFace** dataset [Zhang et al., 2017] under a non-commercial license, contains images with one primary subject and were annotated for age (continuous), gender (Female/Male), and ethnicity (White/Black/Asian/Indian/Others) by an algorithm, then checked by human annotators.

For each of the datasets, we randomly selected a subset of images for our evaluation. We capped the number of images from each intersectional identity at 1,500 as an attempt to reduce the effect of highly imbalanced datasets. We include a total of 66,662 images with 14,919 images from Adience; 21,444 images from CCD; 8,194 images from MIAP; and 22,105 images from UTKFace. The full breakdown of totals of images from each group can be found in Section A.1.

Each image was corrupted a total of 75 times, per the ImageNet-C protocol with the main 15 corruptions each with 5 severity levels. Examples of these corruptions can be seen in Figure 1. This resulted in a total of 5,066,312 images (including the original clean ones) which were each passed through the AWS, Azure, and Google Cloud Platform (GCP) face analysis systems. A detailed description of which API settings were selected can be found in Appendix C. The API calls were conducted between 19 May and 29 May 2021. Images were processed and stored within AWS’s cloud using S3 and EC2. The total cost of the experiments was \$17,507.55 and a breakdown of costs can be found in Appendix D.

Evaluation Metrics. We evaluate the error of the face systems. Since none of the chosen datasets have ground truth face bounding boxes, we compare the number of detected faces from the clean image to the number of faces detected in a corrupted image, using the former as ground truth.

Our main metric is the relative error in the number of faces a system detects after corruption; this metric has been used in other facial processing benchmarks [Jain and Parsheera, 2021]. Measuring error in this way is in some sense incongruous with the object detection nature of the APIs. However, none of the data in our datasets have bounding boxes for each face. This means that we cannot calculate precision metrics as one would usually do with other detection tasks. To overcome this, we hand-annotated bounding boxes for each face in 772 (1.2% of the dataset) random images from the dataset. We then calculated per-image precision scores (with an intersection over union of 0.5) and per-image relative error in face counts and we find a Pearson’s correlation of 0.91 (with $p < 0.001$). This high correlation indicates that the proxy is sufficient to be used in this benchmark in the absence of fully annotated bounding boxes.

This error is calculated for each image. Specifically, we first pass every clean, uncorrupted image through the commercial system’s API. Then, we measure the number of detected faces, i.e., length of the system’s response, and treat this number as the ground truth. Subsequently, we compare the number of detected faces for a corrupted version of that image. If the two face counts are not the same, then we call that an error. We refer to this as the *relative corruption error*. For each clean image, i , from dataset d , and each corruption c which produces a corrupted image $\hat{i}_{c,s}$ with severity s , we compute the relative corruption error for system r as

$$rCE_{c,s}^{d,r}(\hat{i}_{c,s}) := \begin{cases} 1, & \text{if } l_r(i) \neq l_r(\hat{i}_{c,s}) \\ 0, & \text{if } l_r(i) = l_r(\hat{i}_{c,s}) \end{cases}$$

where l_r computes the number of detected faces, i.e., length of the response, from face detection system r when given an image. Often the super- and subscripts are omitted when they are obvious.

Our main metric, relative error, aligns with that of the ImageNet-C benchmark. We report mean relative corruption error ($mrCE$) defined as taking the average of rCE across some relative set of categories. In our experiments, depending on the context, we might have any of the following categories: face systems, datasets, corruptions, severities, age presentation, gender presentation, Fitzpatrick rating, and ambient lighting. For example, we might report the relative mean corruption error when averaging across demographic groups; the mean corruption error for Azure on the UTK dataset for each age group a is $mrCE_a = \frac{1}{15} \frac{1}{5} \sum_{c,s} rCE_{c,s,a}^{UTK,Azure}$. The subscripts on $mrCE$ are omitted when it is obvious what their value is in whatever context they are presented.

Finally, we also investigate the significance of whether the $mrCE$ for two groups are equal. For example, our first question is whether the two commercial systems (AWS and Azure) have comparable $mrCE$ overall. To do this, we report the raw $mrCE$; these frequency or empiric probability statistics offer much insight into the likelihood of error. But we also indicate the statistical significance at $\alpha = 0.05$ determined by logistic regressions for the appropriate variables and interactions. For each

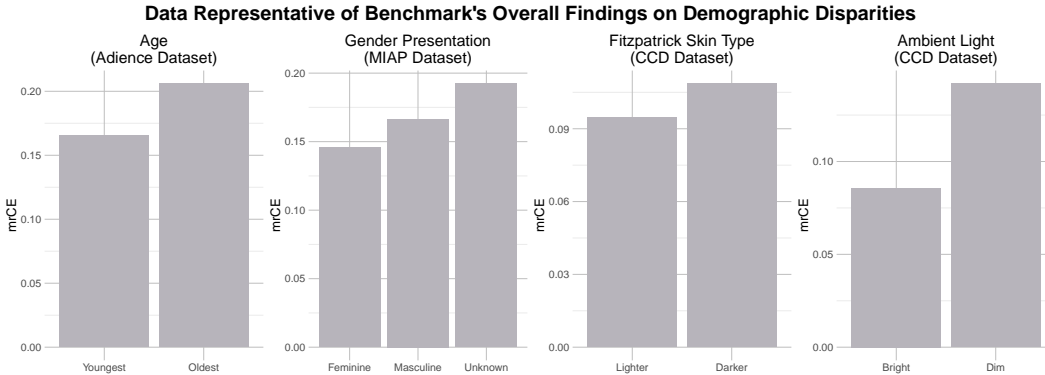


Figure 2: There are disparities in all of the demographics included in this study; we show representative evidence for each demographic on different datasets. On the left, we see (using Adience as an exemplar) that the oldest two age groups are roughly 25% more error prone than the youngest two groups. Using MIAP as an exemplar, masculine presenting subjects are 20% more error prone than feminine. On the CCD dataset, we find that individuals with Fitzpatrick scales IV-VI have a roughly 25% higher chance of error than lighter skinned individuals. Finally, dimly lit individuals are 60% more likely to have errors.

claim of significance, regression tables can be found in the appendix. Accordingly, we discuss the odds or odds ratio of relevant features. See Appendix B for a detailed example. Finally, each claim we make for an individual dataset or service is backed up with statistical rigor through the logistic regressions. Each claim we make across datasets is done by looking at the trends in each dataset and are inherently qualitative.

What is not included in this study. There are three main things that this benchmark does not address. First, we do not examine cause and effect. We report inferential statistics without discussion of what generates them. Second, we only examine the types of algorithmically generated natural noise present in the 15 corruptions. We speak narrowly about robustness to these corruptions or perturbations. We explicitly do not study or measure robustness to other types of changes to images, for instance adversarial noise, camera dimensions, etc. Finally, we do not investigate algorithmic training. We do not assume any knowledge of how the commercial system was developed or what training procedure or data were used.

Social Context. The central analysis of this benchmark relies on socially constructed concepts of gender presentation and the related concepts of race and age. While this benchmark analyzes phenotypal versions of these from metadata on ML datasets, it would be wrong to interpret our findings absent a social lens of what these demographic groups mean inside a society. We guide the reader to Benthall and Haynes [2019] and Hanna et al. [2020] for a look at these concepts for race in machine learning, and Hamidi et al. [2018] and Keyes [2018] for similar looks at gender.

4 Benchmark Results

We now report the main results of our benchmark, a synopsis of which is in Figure 2. Our main results are derived from Table 6 which report one regression for each dataset. Each regression includes all demographic variables and each variable is normalized for consistency across the datasets. Overall, we find that photos of individuals who are *older*, *masculine presenting*, *darker skinned*, or are *dimly lit* are more susceptible to errors than their counterparts. We see that each of these conclusions are consistent across datasets except that UTKFace has masculine presenting individuals as performing better than feminine presenting.

4.1 System Performance

We plot $mrCE$ for each dataset and service in Figure 3; the difference between services is statistically significant for each dataset and each service. The only consistent pattern is that GCP is always worse than Azure. These corruption errors should be compared to the clean errors which are very much less than 1%. For comparison, the lowest $mrCE$ from Figure 3 is 7% for corrupted images. Thus, these corruptions are very significantly impacting the performance of these systems.

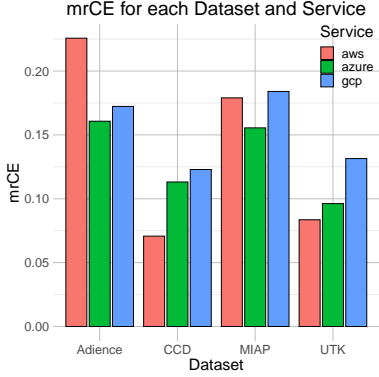


Figure 3: Overall performance differences for each dataset and service

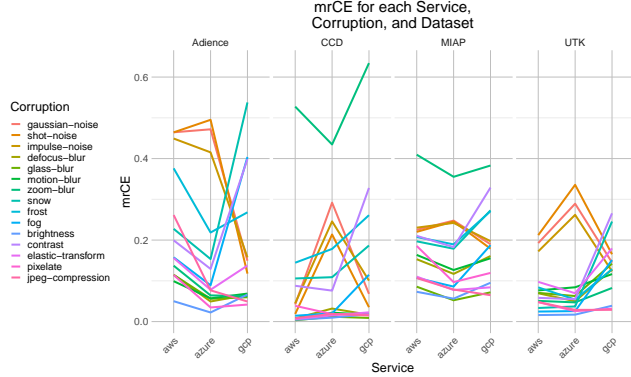


Figure 4: A comparison of mrCE for each corruption across each dataset and service.

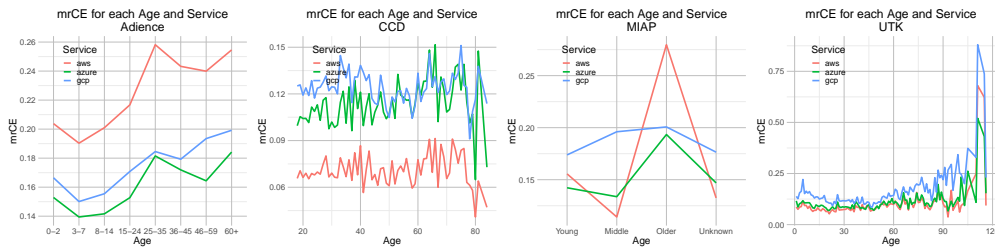


Figure 5: Each figure depicts the mrCE across ages. Each line depicts a commercial system. Age is a categorical variable for Adience and MIAP but a numeric for CCD and UTKFace.

4.2 Noise corruptions are the most difficult

Recall that there are four types of ImageNet-C corruptions: noise, blur, weather, and digital. From Figure 4, we observe that the noise corruptions are markedly some of the most difficult corruptions for Azure to handle across the datasets, whereas GCP has better performance on noise corruptions than Azure and AWS. Though we can only stipulate, these differences might stem from pre-processing steps that each service takes before processing their image. GCP might have a robust noise pre-processing step, which would account for their superior performance with these corruptions.

The zoom blur corruption proves particularly difficult on the CCD and MIAP datasets, though Azure is significantly better than AWS and GCP on both datasets. We also note that all corruptions for all datasets and commercial systems are significantly different from zero. Further details can be found by examining Figure 4 and Appendix Tables 6-10.

4.2.1 Comparison to ImageNet-C results

We compare the Hendrycks and Dietterich [2019] findings to our experiments. We recreate Figure 3 from their paper with more current results for recent models since their paper was published, as well as the addition of our findings; see Figure 8. This figure reproduces their metric, mean corruption error and relative mean corruption error. From this figure, we can conclude that our results are very highly in-line with the predictions from the previous data. This indicates that, even with highly accurate models, accuracy is a strong predictor of robustness.

We also examined the corruption-specific differences between our findings (with face data) and that of the original paper (with ImageNet data). We find that while ImageNet datasets are most susceptible to blurs and digital corruptions, facial datasets are most susceptible to noise corruptions, zoom blur, and weather. These qualitative differences deserve future study.

4.3 Errors increase on older subjects

We observe a significant impact of age on mrCE; see Figure 5. In every dataset and every commercial system (Appendix Tables 6-10), we see that older subjects have significantly higher error rates.

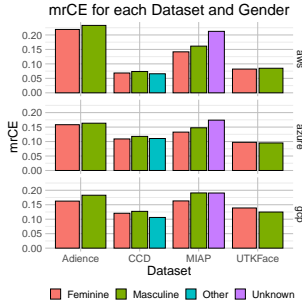


Figure 6: Observe that on all datasets, except for UTKFace, feminine presenting individuals are more robust than masculine.

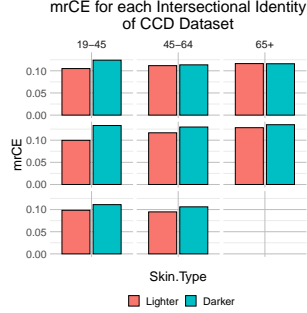


Figure 7: In all intersectional identities, darker skinned individuals are less robust than those who are lighter skinned.

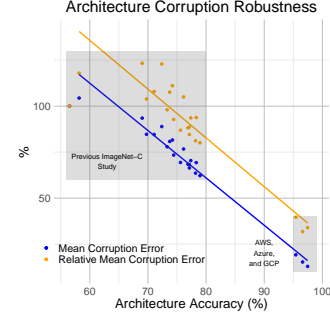


Figure 8: Recreation of Figure 3 from Hendrycks and Dietterich [2019] with contemporary results and the addition of our findings.

On the Adience dataset (Table 7), the odds of error for the oldest group is 31% higher than that of the youngest group. Interestingly, the shape of the $mrCE$ curves across the age groups is similar for each service. For the MIAP dataset (Table 9), the age disparity is very pronounced. In AWS for instance, we see a 145% increase in error for the oldest individuals. The overall odds ratio between the oldest and youngest is 1.383.

The CCD and UTKFace datasets have numeric age. Analyzing the regressions indicates that for every increase of 10 years, there is a 2.3% increase in the likelihood of error on the CCD data and 2.7% increase for UTKFace data.

4.4 Masculine presenting individuals have more errors than feminine presenting

Across all datasets except UTKFace, we find that feminine presenting individuals have lower errors than masculine presenting individuals. See Figure 6. On Adience, feminine individuals have 18.8% $mrCE$ whereas masculine have 19.8%. On CCD, the $mrCE$ s are 8.9% and 9.6% respectively. On the MIAP dataset, the $mrCE$ values are 13.7% and 15.4% respectively. On the UTKFace, both gender presentations have around 9.0% $mrCE$ (non statistically significant difference).

Stepping outside the gender binary, we have two insights into this from these data. In the CCD dataset, the subjects were asked to self-identify their gender. Two individuals selected Other and 62 others did not provide a response. Those two who chose outside the gender binary have a $mrCE$ of 4.9%. When we include those individuals without gender labels, their $mrCE$ is 8.8% and not significantly different from the feminine presenting individuals.

The other insight comes from the MIAP dataset where subjects were rated on their perceived gender presentation by crowdworkers; options were “Predominantly Feminine”, “Predominantly Masculine”, and “Unknown”. For those “Unknown”, the overall $mrCE$ is 19.3%. The creators of the dataset automatically set the gender presentation of those with an age presentation of “Young” to be “Unknown”. The $mrCE$ of those annotations which are not “Young” and have an “Unknown” gender presentation raises to 19.9%. One factor that might contribute to this phenomenon is that individuals with an “Unknown” gender presentation might have faces that are occluded or are small in the image. Further work should be done to explore the causes of this discrepancy.

4.5 Dark skinned subjects have more errors across age and gender identities

We analyze data from the CCD dataset which has ratings for each subject on the Fitzpatrick scale. As is customary in analyzing these ratings, we split the six Fitzpatrick values into two: Lighter (for ratings I-III) and Darker for ratings (IV-VI). The main intersectional results are reported in Figure 7.

The overall $mrCE$ for lighter and darker skin types are 8.5% and 9.7% respectively, a 15% increase for the darker skin type. We also see a similar trend in the intersectional identities available in the CCD metadata (age, gender, and skin type). We see that in every identity (except for 45-64 year old and Feminine) the darker skin type has statistically significant higher error rates. This difference is particularly stark in 19-45 year old, masculine subjects. We see a 35% increase in errors for the darker skin type subjects in this identity compared to those with lighter skin types. For every 20

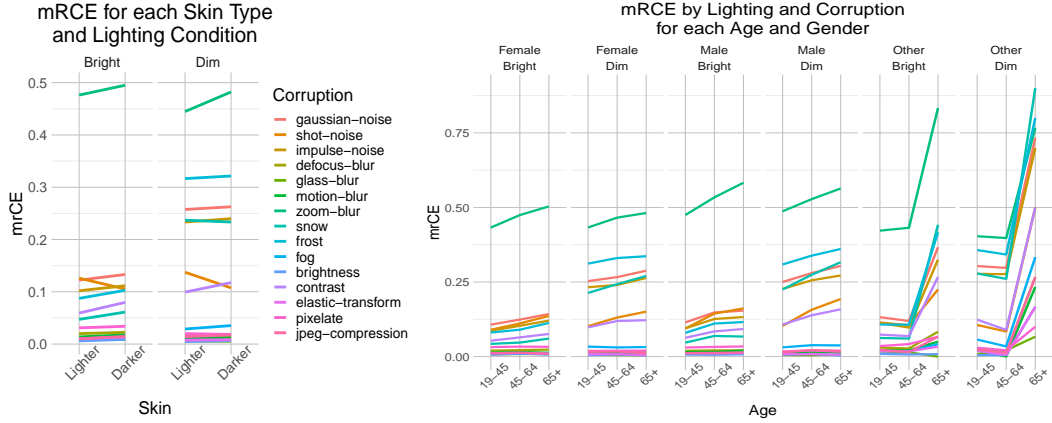


Figure 9: (Left) $mrCE$ is plotted for each corruption by the intersection of lighting condition and skin type. (Right) the same is plotted by the intersection of age, gender, and lighting. Observe that for both skin types, all genders, and all ages, the dimly lit environment increases the error rates.

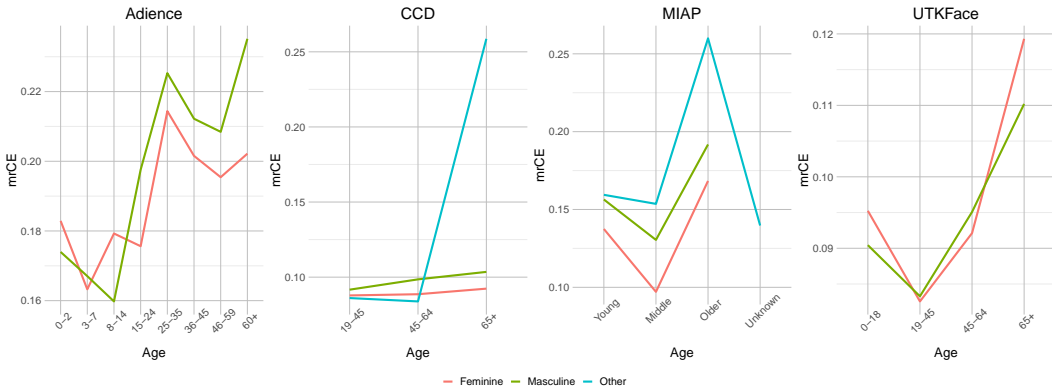


Figure 10: For each dataset, the $mrCE$ is plotted across age groups. Each gender is represented and indicates how gender disparities change across the age groups.

errors on a light skinned, masculine presenting individual between 18 and 45, there are 27 errors for dark skinned individuals of the same category.

4.6 Dim lighting conditions has the most severe impact on errors

Using lighting condition information from the CCD dataset, we observe the $mrCE$ is substantially higher in dimly lit environments: 12.5% compared to 7.8% in bright environments. See Figure 9.

Across the board, we generally see that the disparity in demographic groups decreases between bright and dimly lit environments. For example, the odds ratio between dark and light skinned subjects is 1.09 for bright environments, but decreases to 1.03 for dim environments. This is true for age groups (e.g., odds ratios 1.150 (bright) vs 1.078 (dim) for 45-64 compared to 19-45; 1.126 (bright) vs 1.060 (dim) for Males compared to Females). This is not true for individuals with gender identities as Other or omitted – the disparity increases (1.053 (bright) vs 1.145 (dim) with Females as the reference).

In Figure 9 we observe the lighting differences for different intersectional identities across corruptions. We continue to see zoom blur as the most challenging corruption. Interestingly, the noise and some weather corruptions have a large increase in their errors in dimly lit environments across intersectional identities whereas many of the other corruptions do not.

4.7 Older subjects have higher gender error disparities

We plot in Figure 10 the $mrCE$ for each dataset across age with each gender group plotted separately. From this, we can note that on the CCD and MIAP dataset, the masculine presenting group is always less robust than the feminine. On the CCD dataset, the disparity between the two groups increases

as the age increases (odds ratio of 1.040 for 19-45 raises to 1.138 for 65+). On the MIAP dataset, the odds ratio is greatest between masculine and feminine for the middle age group (1.395). The disparities between the ages also increases from feminine to masculine to unknown gender identities.

On the Adience and UTKFace datasets, we see that the feminine presenting individuals sometimes have higher error rates than masculine presenting subjects. Notably, the most disparate errors in genders on these datasets occurs at the oldest categories, following the trend from the other datasets.

5 Gender and Age Estimation Analysis

We briefly overview results from evaluating AWS’s age and gender estimation commercial systems. Further analysis can be found in Appendices F and G.

5.1 Gender estimation is at least twice as susceptible to corruptions as face detection

The use of automated gender estimates in ML is a controversial topic. Trans and gender queer individuals are often ignored in ML research, though there is a growing body of research that aims to use these technologies in an assistive way as well [e.g., Ahmed, 2019, Chong et al., 2021]. To evaluate gender estimation, we only use CCD as the subjects of these photos voluntarily identified their gender. We omit from the analysis any individual who either did not choose to give their gender or falls outside the gender binary because AWS only estimates Male and Female.

AWS misgenders 9.1% of the clean images but 21.6% of the corrupted images. Every corruption performs worse on gender estimation than *mrCE*. Two corruptions (elastic transform and glass blur) do not have statistically different errors from the clean images. All the others do, with the most significant being zoom blur, Gaussian noise, impulse noise, snow, frost, shot noise, and contrast. Zoom blur’s probability of error is 61% and Gaussian noise is 32%. This compares to *mrCE* values of 43% and 29% respectively. See Appendix F for further analysis.

5.2 Corrupted images error in their age predictions by 40% more than clean images

To estimate Age, AWS returns an upper and lower age estimation. Following their own guidelines on face detection [AWS], we use the mid-point of these numbers as a approximate estimate. On average, the estimation is 8.3 years away from the actual age of the subject for corrupted data, this compares to 5.9 years away for clean data. See Appendix G for further analysis.

6 Conclusion

This benchmark has evaluated three leading commercial facial detection and analysis systems for their robustness against common natural noise corruptions. Using the 15 ImageNet-C corruptions, we measured the relative mean corruption error as measured by comparing the number of faces detected in a clean and corrupted image. We used four academic datasets which included demographic detail.

We observed through our analysis that there are significant demographic disparities in the likelihood of error on corrupted data. We found that older individuals, masculine presenting individuals, those with darker skin types, or in photos with dim ambient light all have higher errors ranging from 20-60%. We also investigated questions of intersectional identities finding that darker males have the highest corruption errors. As for age and gender estimation, corruptions have a significant and sizeable impact on the system’s performance; gender estimation is more than twice as bad on corrupted images as it is on clean images; age estimation is 40% worse on corrupted images.

Future work could explore other metrics for evaluating face detection systems when ground truth bounding boxes are not present. While we considered the length of response on clean images to be ground truth, it could be viable to treat the clean image’s bounding boxes as ground truth and measure deviations therefrom when considering questions of robustness. Of course, this would require a transition to detection-based metrics like precision, recall, and *F*-measure.

We do not explore questions of causation in this benchmark. We do not have enough different datasets or commercial systems to probe this question through regressions or mixed effects modeling. We do note that there is work that examines causation questions with such methods like that of Best-Rowden and Jain [2017] and Cook et al. [2019]. With additional data and under similar benchmarking protocols, one could start to examine this question. However, the black-box nature of commercial systems presents unique challenges to this endeavor.

Acknowledgments and Disclosure of Funding

This research was supported in part by NSF CAREER Award IIS-1846237, NSF D-ISR Award #2039862, NSF Award CCF-1852352, NIH R01 Award NLM-013039-01, NIST MSE Award #20126334, DARPA GARD #HR00112020007, and DoD WHS Award #HQ003420F0035. We thank Candice Schumann for answering questions related to the MIAP dataset, as well as Aurelia Augusta, Brian Brubach, Valeria Cherepanova, Vedant Nanda, Aviva Prins, Liz O’Sullivan, Neehar Peri, Candice Schumann for advice and feedback.

References

- Guidelines on face attributes. <https://docs.aws.amazon.com/rekognition/latest/dg/guidance-face-attributes.html>. Accessed: 2021-08-29.
- E. Adeli, Q. Zhao, A. Pfefferbaum, E. V. Sullivan, L. Fei-Fei, J. C. Niebles, and K. M. Pohl. Representation learning with statistical independence to mitigate bias. In *Proceedings of the IEEE/CVF Winter Conference on Applications of Computer Vision*, pages 2513–2523, 2021.
- A. Agarwal, A. Beygelzimer, M. Dudik, J. Langford, and H. Wallach. A reductions approach to fair classification. In *Proceedings of the 35th International Conference on Machine Learning*, volume 80, pages 60–69, 2018. URL <http://proceedings.mlr.press/v80/agarwal18a.html>.
- A. A. Ahmed. Bridging social critique and design: Building a health informatics tool for transgender voice. In *Extended Abstracts of the 2019 CHI Conference on Human Factors in Computing Systems*, pages 1–4, 2019.
- S. Barocas, M. Hardt, and A. Narayanan. *Fairness and Machine Learning*. fairmlbook.org, 2019. <http://www.fairmlbook.org>.
- S. Benthall and B. D. Haynes. Racial categories in machine learning. In *Proceedings of the conference on fairness, accountability, and transparency*, pages 289–298, 2019.
- L. Best-Rowden and A. K. Jain. Longitudinal study of automatic face recognition. *IEEE transactions on pattern analysis and machine intelligence*, 40(1):148–162, 2017.
- A. Beutel, J. Chen, Z. Zhao, and E. H. Chi. Data decisions and theoretical implications when adversarially learning fair representations. *arXiv preprint arXiv:1707.00075*, 2017.
- J. Buolamwini and T. Gebru. Gender shades: Intersectional accuracy disparities in commercial gender classification. In *Proceedings of the 1st Conference on Fairness, Accountability and Transparency*, volume 81, pages 77–91, 2018. URL <http://proceedings.mlr.press/v81/buolamwini18a.html>.
- V. Cherepanova, M. Goldblum, H. Foley, S. Duan, J. P. Dickerson, G. Taylor, and T. Goldstein. Lowkey: leveraging adversarial attacks to protect social media users from facial recognition. In *International Conference on Learning Representations (ICLR)*, 2021.
- T. Chong, N. Maudet, K. Harima, and T. Igarashi. Exploring a makeup support system for transgender passing based on automatic gender recognition. In *Proceedings of the 2021 CHI Conference on Human Factors in Computing Systems*, pages 1–13, 2021.
- A. Chouldechova and A. Roth. The frontiers of fairness in machine learning. *arXiv preprint arXiv:1810.08810*, 2018.
- C. M. Cook, J. J. Howard, Y. B. Sirotin, J. L. Tipton, and A. R. Vemury. Demographic effects in facial recognition and their dependence on image acquisition: An evaluation of eleven commercial systems. *IEEE Transactions on Biometrics, Behavior, and Identity Science*, 1(1):32–41, 2019.
- W. Derringer. A surveillance net blankets china’s cities, giving police vast powers. *The New York Times*, Dec. 17 2019. URL <https://www.nytimes.com/2019/12/17/technology/china-surveillance.html>.

- E. Diana, W. Gill, M. Kearns, K. Kenthapadi, and A. Roth. Convergent algorithms for (relaxed) minimax fairness. *arXiv preprint arXiv:2011.03108*, 2020.
- M. Donini, L. Oneto, S. Ben-David, J. Shawe-Taylor, and M. Pontil. Empirical risk minimization under fairness constraints. In *Proceedings of the 32nd International Conference on Neural Information Processing Systems, NIPS'18*, page 2796–2806, 2018.
- C. Dwork, M. Hardt, T. Pitassi, O. Reingold, and R. Zemel. Fairness through awareness. In *Proceedings of the 3rd Innovations in Theoretical Computer Science Conference, ITCS '12*, page 214–226, New York, NY, USA, 2012. Association for Computing Machinery. ISBN 9781450311151. doi: 10.1145/2090236.2090255. URL <https://doi.org/10.1145/2090236.2090255>.
- H. Edwards and A. J. Storkey. Censoring representations with an adversary. In *4th International Conference on Learning Representations, ICLR 2016, San Juan, Puerto Rico, May 2-4, 2016, Conference Track Proceedings*, 2016. URL <http://arxiv.org/abs/1511.05897>.
- E. Eidinger, R. Enbar, and T. Hassner. Age and gender estimation of unfiltered faces. *IEEE Transactions on Information Forensics and Security*, 9(12):2170–2179, 2014.
- H. El Khiyari and H. Wechsler. Face verification subject to varying (age, ethnicity, and gender) demographics using deep learning. *Journal of Biometrics and Biostatistics*, 7(323):11, 2016.
- M. Feldman, S. A. Friedler, J. Moeller, C. Scheidegger, and S. Venkatasubramanian. Certifying and removing disparate impact. In *Knowledge Discovery and Data Mining*, pages 259–268, 2015.
- T. B. Fitzpatrick. The validity and practicality of sun-reactive skin types i through vi. *Archives of dermatology*, 124(6):869–871, 1988.
- C. Garvie. *The perpetual line-up: Unregulated police face recognition in America*. Georgetown Law, Center on Privacy & Technology, 2016.
- N. Goel, M. Yaghini, and B. Faltings. Non-discriminatory machine learning through convex fairness criteria. *Proceedings of the AAAI Conference on Artificial Intelligence*, 32(1), 2018. URL <https://ojs.aaai.org/index.php/AAAI/article/view/11662>.
- Google. How google uses pattern recognition to make sense of images. <https://policies.google.com/technologies/pattern-recognition?hl=en-US>, 2021. Accessed: 2021-06-07.
- P. Grother, M. Ngan, and K. Hanaoka. *Face Recognition Vendor Test (FVRT): Part 3, Demographic Effects*. National Institute of Standards and Technology, 2019.
- D. Gutman. King County Council bans use of facial recognition technology by Sheriff’s Office, other agencies. *The Seattle Times*, June 2021. URL <https://www.seattletimes.com/seattle-news/politics/king-county-council-bans-use-of-facial-recognition-technology-by-sheriffs-office-other-agencies/>.
- F. Hamidi, M. K. Scheuerman, and S. M. Branham. Gender recognition or gender reductionism? the social implications of embedded gender recognition systems. In *Proceedings of the 2018 chi conference on human factors in computing systems*, pages 1–13, 2018.
- A. Hanna, E. Denton, A. Smart, and J. Smith-Loud. Towards a critical race methodology in algorithmic fairness. In *Proceedings of the 2020 conference on fairness, accountability, and transparency*, pages 501–512, 2020.
- M. Hardt, E. Price, E. Price, and N. Srebro. Equality of opportunity in supervised learning. In *Advances in Neural Information Processing Systems*, volume 29, pages 3315–3323, 2016. URL <https://proceedings.neurips.cc/paper/2016/file/9d2682367c3935defcb1f9e247a97c0d-Paper.pdf>.
- W. Hartzog. The secretive company that might end privacy as we know it. *The New York Times*, Jan. 18 2020. URL <https://www.nytimes.com/2020/01/18/technology/clearview-privacy-facial-recognition.html>.

- C. Hazirbas, J. Bitton, B. Dolhansky, J. Pan, A. Gordo, and C. C. Ferrer. Towards measuring fairness in ai: the casual conversations dataset. *arXiv preprint arXiv:2104.02821*, 2021.
- D. Hendrycks and T. Dietterich. Benchmarking neural network robustness to common corruptions and perturbations. 2019.
- H. Hosseini, B. Xiao, and R. Poovendran. Google’s cloud vision API is not robust to noise. In *2017 16th IEEE international conference on machine learning and applications (ICMLA)*, pages 101–105. IEEE, 2017.
- G. Jain and S. Parsheera. 1.4 billion missing pieces? auditing the accuracy of facial processing tools on indian faces. *First Workshop on Ethical Considerations in Creative applications of Computer Vision*, 2021.
- S. Kantayya. Coded bias, 2020. Feature-length documentary.
- O. Keyes. The misgendering machines: Trans/hci implications of automatic gender recognition. *Proceedings of the ACM on human-computer interaction*, 2(CSCW):1–22, 2018.
- B. F. Klare, M. J. Burge, J. C. Klontz, R. W. V. Bruegge, and A. K. Jain. Face recognition performance: Role of demographic information. *IEEE Transactions on Information Forensics and Security*, 7(6): 1789–1801, 2012.
- P. Lahoti, A. Beutel, J. Chen, K. Lee, F. Prost, N. Thain, X. Wang, and E. H. Chi. Fairness without demographics through adversarially reweighted learning. *arXiv preprint arXiv:2006.13114*, 2020.
- S. Lohr. Facial recognition is accurate, if you’re a white guy. *New York Times*, 9, 2018.
- D. Madras, E. Creager, T. Pitassi, and R. S. Zemel. Learning adversarially fair and transferable representations. In *Proceedings of the 35th International Conference on Machine Learning, ICML 2018, Stockholmsmässan, Stockholm, Sweden, July 10-15, 2018*, volume 80 of *Proceedings of Machine Learning Research*, pages 3381–3390. PMLR, 2018. URL <http://proceedings.mlr.press/v80/madras18a.html>.
- J. Marson and B. Forrest. Armed low-cost drones, made by turkey, reshape battlefields and geopolitics. *The Wall Street Journal*, Jun 2021. URL <https://www.wsj.com/articles/armed-low-cost-drones-made-by-turkey-reshape-battlefields-and-geopolitics-11622727370>.
- N. Martinez, M. Bertran, and G. Sapiro. Minimax pareto fairness: A multi objective perspective. In *Proceedings of the 37th International Conference on Machine Learning*, volume 119, pages 6755–6764, 2020. URL <http://proceedings.mlr.press/v119/martinez20a.html>.
- V. Nanda, S. Dooley, S. Singla, S. Feizi, and J. P. Dickerson. Fairness through robustness: Investigating robustness disparity in deep learning. In *Proceedings of the 2021 ACM Conference on Fairness, Accountability, and Transparency*, pages 466–477, 2021.
- A. J. O’Toole, P. J. Phillips, X. An, and J. Dunlop. Demographic effects on estimates of automatic face recognition performance. *Image and Vision Computing*, 30(3):169–176, 2012.
- M. Padala and S. Gujar. Fnnc: Achieving fairness through neural networks. In *Proceedings of the Twenty-Ninth International Joint Conference on Artificial Intelligence, IJCAI-20*, pages 2277–2283. International Joint Conferences on Artificial Intelligence Organization, 7 2020. doi: 10.24963/ijcai.2020/315. URL <https://doi.org/10.24963/ijcai.2020/315>.
- P. J. Phillips, W. T. Scruggs, A. J. O’Toole, P. J. Flynn, K. W. Bowyer, C. L. Schott, and M. Sharpe. Fvt 2006 and ice 2006 large-scale results. *National Institute of Standards and Technology, NISTIR*, 7408(1):1, 2007.
- P. J. Phillips, J. R. Beveridge, B. A. Draper, G. Givens, A. J. O’Toole, D. S. Bolme, J. Dunlop, Y. M. Lui, H. Sahibzada, and S. Weimer. An introduction to the good, the bad, & the ugly face recognition challenge problem. In *2011 IEEE International Conference on Automatic Face & Gesture Recognition (FG)*, pages 346–353. IEEE, 2011.

- N. Quadrianto, V. Sharmanska, and O. Thomas. Discovering fair representations in the data domain. In *IEEE Conference on Computer Vision and Pattern Recognition, CVPR 2019, Long Beach, CA, USA, June 16-20, 2019*, pages 8227–8236. Computer Vision Foundation / IEEE, 2019. doi: 10.1109/CVPR.2019.00842. URL http://openaccess.thecvf.com/content_CVPR_2019/html/Quadrianto_Discovering_Fair_Representations_in_the_Data_Domain_CVPR_2019_paper.html.
- I. D. Raji and J. Buolamwini. Actionable auditing: Investigating the impact of publicly naming biased performance results of commercial ai products. In *Proceedings of the 2019 AAAI/ACM Conference on AI, Ethics, and Society*, pages 429–435, 2019.
- H. J. Ryu, H. Adam, and M. Mitchell. Inclusivefacenet: Improving face attribute detection with race and gender diversity. *arXiv preprint arXiv:1712.00193*, 2018.
- Y. Savani, C. White, and N. S. Govindarajulu. Intra-processing methods for debiasing neural networks. In *Proceedings of Advances in Neural Information Processing Systems*, 2020.
- C. Schumann, C. R. Pantofaru, S. Ricco, U. Prabhu, and V. Ferrari. A step toward more inclusive people annotations for fairness. In *Proceedings of the AAAI/ACM Conference on AI, Ethics, and Society*, 2021.
- S. Shan, E. Wenger, J. Zhang, H. Li, H. Zheng, and B. Y. Zhao. Fawkes: Protecting privacy against unauthorized deep learning models. In *29th {USENIX} Security Symposium ({USENIX} Security 20)*, pages 1589–1604, 2020.
- N. Singer. Microsoft urges congress to regulate use of facial recognition. *The New York Times*, 2018.
- R. Singh, A. Agarwal, M. Singh, S. Nagpal, and M. Vatsa. On the robustness of face recognition algorithms against attacks and bias. In *Proceedings of the AAAI Conference on Artificial Intelligence*, volume 34, pages 13583–13589, 2020.
- M. Wang and W. Deng. Mitigating bias in face recognition using skewness-aware reinforcement learning. In *Proceedings of the IEEE/CVF Conference on Computer Vision and Pattern Recognition*, pages 9322–9331, 2020.
- T. Wang, J. Zhao, M. Yatskar, K.-W. Chang, and V. Ordonez. Balanced datasets are not enough: Estimating and mitigating gender bias in deep image representations. In *Proceedings of the IEEE International Conference on Computer Vision*, pages 5310–5319, 2019.
- Z. Wang, K. Qinami, I. C. Karakozis, K. Genova, P. Nair, K. Hata, and O. Russakovsky. Towards fairness in visual recognition: Effective strategies for bias mitigation, 2020.
- K. Weise and N. Singer. Amazon pauses police use of its facial recognition software. *The New York Times*, Jul. 10 2020. URL <https://www.nytimes.com/2020/06/10/technology/amazon-facial-recognition-backlash.html>.
- M. J. Wilber, V. Shmatikov, and S. Belongie. Can we still avoid automatic face detection? In *2016 IEEE Winter Conference on Applications of Computer Vision (WACV)*, pages 1–9. IEEE, 2016.
- M. B. Zafar, I. Valera, M. Gomez Rodriguez, and K. P. Gummadi. Fairness beyond disparate treatment & disparate impact. *Proceedings of the 26th International Conference on World Wide Web*, Apr 2017a. doi: 10.1145/3038912.3052660. URL <http://dx.doi.org/10.1145/3038912.3052660>.
- M. B. Zafar, I. Valera, M. Gomez-Rodriguez, and K. P. Gummadi. Fairness constraints: Mechanisms for fair classification. In *Proceedings of the 20th International Conference on Artificial Intelligence and Statistics, AISTATS 2017, 20-22 April 2017, Fort Lauderdale, FL, USA*, volume 54 of *Proceedings of Machine Learning Research*, pages 962–970. PMLR, 2017b. URL <http://proceedings.mlr.press/v54/zafar17a.html>.
- M. B. Zafar, I. Valera, M. Gomez-Rodriguez, and K. P. Gummadi. Fairness constraints: A flexible approach for fair classification. *Journal of Machine Learning Research*, 20(75):1–42, 2019. URL <http://jmlr.org/papers/v20/18-262.html>.

- R. Zemel, Y. Wu, K. Swersky, T. Pitassi, and C. Dwork. Learning fair representations. volume 28 of *Proceedings of Machine Learning Research*, pages 325–333, Atlanta, Georgia, USA, 17–19 Jun 2013. PMLR. URL <http://proceedings.mlr.press/v28/zemel13.html>.
- Z. Zhang, Y. Song, and H. Qi. Age progression/regression by conditional adversarial autoencoder. In *Proceedings of the IEEE conference on computer vision and pattern recognition*, pages 5810–5818, 2017.

A Evaluation Information

A.1 Image Counts

For each dataset, we selected no more than 1,500 images from any intersectional group. The final tallies of how many images from each group can be found in Tables 1, 2, 3, and 4.

A.2 Corruption information

We evaluate 15 corruptions from Hendrycks and Dietterich [2019]: Gaussian noise, shot noise, impulse noise, defocus blur, glass blur, motion blur, zoom blur, snow, frost, fog, brightness, contrast, elastic transforms, pixelation, and jpeg compressions. Each corruption is described in the Hendrycks and Dietterich [2019] paper as follows:

The first corruption type is Gaussian noise. This corruption can appear in low-lighting conditions. Shot noise, also called Poisson noise, is electronic noise caused by the discrete nature of light itself. Impulse noise is a color analogue of salt-and-pepper noise and can be caused by bit errors. Defocus blur occurs when an image is out of focus. Frosted Glass Blur appears with “frosted glass” windows or panels. Motion blur appears when a camera is moving quickly. Zoom blur occurs when a camera moves toward an object rapidly. Snow is a visually obstructive form of precipitation. Frost forms when lenses or windows are coated with ice crystals. Fog shrouds objects and is rendered with the diamond-square algorithm. Brightness varies with daylight intensity. Contrast can be high or low depending on lighting conditions and the photographed object’s color. Elastic transformations stretch or contract small image regions. Pixelation occurs when upsampling a lowresolution image. JPEG is a lossy image compression format which introduces compression artifacts.

The specific parameters for each corruption can be found in the project’s github at the corruptions file: https://github.com/dooleys/Robustness-Disparities-in-Commercial-Face-Detection/blob/main/code/imagenet_c_big/corruptions.py.

B Metric Discussion

Our use of relative error is slightly adapted from ImageNet-C inasmuch that in that paper, they were measuring top-1 error of classification systems. However, the concept is identical. Consequently, it is linguistically best for our measure to be *mean relative* corruption error, whereas ImageNet-C reports the *mean relative* corruption error. This symmantic difference is attributed to when we take our average versus when the ImageNet-C protocol does.

B.1 Response Example

Our main metric, $mrCE$ relies on the computing the number of detected faces, i.e., length of a response, l_r , from an API service. We explicitly give an example of this here.

An example response from an API service is below has one face detected:

```
[
  {
    "face_rectangle": {
      "width": 601,
      "height": 859,
      "left": 222,
      "top": 218
    }
  }
]
```

An example response from an API service is below has two faces detected:

```
[
  {
    "face_rectangle": {
      "width": 601,
      "height": 859,
      "left": 222,
```

```

    "top": 218
  },
  {
    "face_rectangle": {
      "width": 93,
      "height": 120,
      "left": 10,
      "top": 39
    }
  }
]

```

B.2 Metric Example

Let us consider an example. Assume we were testing the question of whether there is a difference in error rates for different eye colors: (Grey, Hazel, and Brown). Across all the corrupted data, we might see that rCE is 0.12, 0.21, and 0.23 for Grey, Hazel, and Brown respectively. Recall that the odds of an event with likelihood p is reported as $p/(1-p)$. So the odds of error for each eye color is 0.14, 0.27, and 0.30 respectively. Our logistic regression would be written as $rCE = \beta_0 + \beta_1\text{Hazel} + \beta_2\text{Brown}$, with Hazel and Brown being indicator variables. After fitting our regression, we might see that the estimated *odds* coefficients for the intercept is 0.14, for the variable Hazel is 1.93, and for the variable Brown is 2.14; and all the coefficients are significant. This makes sense because the odds of Grey is 0.14, the odds ratio between Hazel and Grey is $0.27/0.14 = 1.93$, and the odds ratio between Brown and Grey is $0.30/0.14 = 2.14$. The significance tells us that the odds (or probability) or error for Grey eyes is significantly different from the odds (or probability) of error for Brown and Hazel eyes. In this example, we can conclude that the odds of error is 2.14 higher for Brown eyes compared to Grey. Put another way, for every 1 error for a Grey eyed person, there would be roughly 2 errors for a Hazel or Brown person. More so, the odds of error for Brown eyes is 114% higher than the odds of error for for Grey eyes.

C API Parameteres

For the AWS DetectFaces API,¹ we selected to have all facial attributes returned. This includes age and gender estimates. We evaluate the performance of these estimates in Section 5. The Azure Face API² allows the user to select one of three detection models. We chose model `detection_03` as it was their most recently released model (February 2021) and was described to have the highest performance on small, side, and blurry faces, since it aligns with our benchmark intention. This model does not return age or gender estimates (though model `detection_01` does).

D Benchmarks Costs

A total breakdown of costs for this benchmark can be found in Table 5.

E Statistical Significance Regressions for rCE

E.1 Main Tables

Regression of $mrCE$ for all variables for the all the datasets with unified demographic variables can be found in Table 6.

Regression of $mrCE$ for all variables for the Adience dataset can be found in Table 7.

Regression of $mrCE$ for all variables for the CCD dataset can be found in Table 8.

Regression of $mrCE$ for all variables for the MIAP dataset can be found in Table 9.

Regression of $mrCE$ for all variables for the UTKFace dataset can be found in Table 10.

¹https://docs.aws.amazon.com/rekognition/latest/dg/API_DetectFaces.html

²<https://westus.dev.cognitive.microsoft.com/docs/services/563879b61984550e40cbb8d/operations/563879b61984550f30395236>

E.1.1 Adience Demographic Interactions

Regression of $mrCE$ for the interaction of Age and Gender for the Adience dataset can be found in Table 11.

E.1.2 CCD Demographic Interactions

Regression of $mrCE$ for the interaction of Lighting and Skin Type for the CCD dataset can be found in Table 12.

Regression of $mrCE$ for the interaction of Lighting and Age for the CCD dataset can be found in Table 13.

Regression of $mrCE$ for the interaction of Lighting and Age (as a numeric variable) for the CCD dataset can be found in Table 14.

Regression of $mrCE$ for the interaction of Lighting and Gender for the CCD dataset can be found in Table 15.

Regression of $mrCE$ for the interaction of Age and Gender for the CCD dataset can be found in Table 16.

Regression of $mrCE$ for the interaction of Age and Skin Type for the CCD dataset can be found in Table 17.

Regression of $mrCE$ for the interaction of Age, Skin Type, and Gender for the CCD dataset can be found in Table 18.

Regression of $mrCE$ for the interaction of Age (as a numeric variable) and Gender for the CCD dataset can be found in Table 19.

Regression of $mrCE$ for the interaction of Age (as a numeric variable) and Skin Type for the CCD dataset can be found in Table 20.

Regression of $mrCE$ for the interaction of Gender and Skin Type for the CCD dataset can be found in Table 21.

E.1.3 MIAP Demographic Interactions

Regression of $mrCE$ for the interaction of Age and Gender for the MIAP dataset can be found in Table 22.

E.1.4 UTKFace Demographic Interactions

Regression of $mrCE$ for the interaction of Age and Gender for the UTKFace dataset can be found in Table 23.

Regression of $mrCE$ for the interaction of Age and Ethnicity for the UTKFace dataset can be found in Table 24.

Regression of $mrCE$ for the interaction of Gender and Ethnicity for the UTKFace dataset can be found in Table 25.

Regression of $mrCE$ for the interaction of Gender and Ethnicity for the UTKFace dataset can be found in Table 25.

F Statistical Significance Regressions for Gender Prediction

Regression of gender estimation for all variables for the all the datasets with unified demographic variables can be found in Table 26.

Regression of gender prediction for all variables for the Adience dataset can be found in Table 27.

Regression of gender estimation for all variables for the CCD dataset can be found in Table 28.

Regression of gender estimation for all variables for the MIAP dataset can be found in Table 29.

Regression of gender estimation for all variables for the UTKFace dataset can be found in Table 30.

G Statistical Significance Regressions for Age Estimation

Regression of Age estimation for all variables for the CCD dataset can be found in Table 31.

Regression of age estimation for all variables for the UTKFace dataset can be found in Table 32.

List of Tables

1	Adience Dataset Counts	20
2	CCD Dataset Counts	21
3	MIAP Dataset Counts	22
4	UTKFace Dataset Counts	23
5	Total Costs of Benchmark	24
6	Main regressions (odds ratio) for the all datasets with unified demographic variables.	25
7	Full regression (odds ratio) for the Adience dataset.	26
8	Full regression (odds ratio) for the CCD dataset.	27
9	Full regression (odds ratio) for the MIAP dataset.	28
10	Full regression (odds ratio) for the UTKFace dataset.	29
11	Interaction (odds ratio) of Age and Gender for the Adience dataset.	30
12	Interaction (odds ratio) of Lighting and Skin Type for the CCD dataset.	31
13	Interaction (odds ratio) of Lighting and Age for the CCD dataset.	32
14	Interaction (odds ratio) of Lighting and Age (as a numeric variable) for the CCD dataset.	33
15	Interaction (odds ratio) of Lighting and Gender for the CCD dataset.	34
16	Interaction (odds ratio) of Age and Gender for the CCD dataset.	35
17	Interaction (odds ratio) of Age and Skin Type for the CCD dataset.	36
18	Interaction (odds ratio) of Age, Skin Type, and Gender for the CCD dataset.	37
19	Interaction (odds ratio) of Age (as a numeric variable) and Gender for the CCD dataset.	38
20	Interaction (odds ratio) of Age (as a numeric variable) and Skin Type for the CCD dataset.	39
21	Interaction (odds ratio) of Gender and Skin Type for the CCD dataset.	40
22	Interaction (odds ratio) of Age and Gender for the MIAP dataset.	41
23	Interaction (odds ratio) of Age and Gender for the UTKFace dataset.	42
24	Interaction (odds ratio) of Age and Ethnicity for the UTKFace dataset.	43
25	Interaction (odds ratio) of Gender and Ethnicity for the UTKFace dataset.	44
26	Gender estimation (odds ratio) for the all datasets with unified demographic variables.	45
27	Gender prediction (odds ratio) for the Adience dataset.	46
28	Gender estimation (odds ratio) for the CCD dataset.	47
29	Gender estimation (odds ratio) for the MIAP dataset.	48
30	Gender estimation (odds ratio) for the UTKFace dataset.	49
31	Age estimation for the CCD dataset.	50
32	Age estimation for the UTKFace dataset.	51

Table 1: Adience Dataset Counts

Age	Gender	Count
0-2	Female	684
	Male	716
3-7	Female	1232
	Male	925
8-14	Female	1353
	Male	933
15-24	Female	1047
	Male	742
25-35	Female	1500
	Male	1500
36-45	Female	1078
	Male	1412
46-59	Female	436
	Male	466
60+	Female	428
	Male	467

Table 2: CCD Dataset Counts

Lighting	Gender	Skin	Age	Count	
Bright	Female	Dark	19-45	1500	
			45-64	1500	
			65+	547	
		Light	19-45	1500	
			45-64	1500	
			65+	653	
		Male	Dark	19-45	1500
				45-64	1500
				65+	384
	Light		19-45	1500	
			45-64	1500	
			65+	695	
	Other		Dark	19-45	368
				45-64	168
				65+	12
	Dim	Female	Dark	19-45	1500
				45-64	670
				65+	100
Light			19-45	642	
			45-64	314	
			65+	131	
Male			Dark	19-45	1500
				45-64	387
				65+	48
		Light	19-45	485	
			45-64	299	
			65+	123	
		Other	Dark	19-45	57
				45-64	26
				65+	3
Light			19-45	27	
			45-64	12	

Table 3: MIAP Dataset Counts

AgePresentation	GenderPresentation	Count
Young	Unknown	1500
Middle	Predominantly Feminine	1500
	Predominantly Masculine	1500
Older	Unknown	561
	Predominantly Feminine	209
	Predominantly Masculine	748
Unknown	Unknown	24
	Predominantly Feminine	250
	Predominantly Masculine	402
	Unknown	1500

Table 4: UTKFace Dataset Counts

Age	Gender	Race	Count
0-18	Female	Asian	555
		Black	161
		Indian	350
		Others	338
		White	987
	Male	Asian	586
		Black	129
		Indian	277
		Others	189
		White	955
19-45	Female	Asian	1273
		Black	1500
		Indian	1203
		Others	575
		White	1500
	Male	Asian	730
		Black	1499
		Indian	1264
		Others	477
		White	1500
45-64	Female	Asian	39
		Black	206
		Indian	146
		Others	22
		White	802
	Male	Asian	180
		Black	401
		Indian	653
		Others	97
		White	1500
65+	Female	Asian	75
		Black	78
		Indian	43
		Others	10
		White	712
	Male	Asian	148
		Black	166
		Indian	91
		Others	5
		White	682

Table 5: Total Costs of Benchmark

Category	Cost
Azure Face Service	\$4,270.58
AWS Rekognition	\$4,270.66
Google Cloud Platform	\$7,230.47
S3	\$1,003.83
EC2	\$475.77
Tax	\$256.24
Total	\$17,507.55

Table 6: Main regressions (odds ratio) for the all datasets with unified demographic variables.

	Dependent variable:			
	rCE			
	Adience (1)	CCD (2)	MIAP (3)	UTKFace (4)
AgeMiddle	1.272 t = 78.398***	1.139 t = 9.183***	0.918 t = -12.127***	0.866 t = -38.599***
AgeOlder	1.359 t = 49.904***	1.461 t = 25.535***	1.383 t = 57.381***	1.328 t = 51.626***
AgeUnknown			0.780 t = -33.288***	
GenderMale	1.076 t = 24.647***	1.129 t = 35.165***	1.187 t = 29.740***	0.953 t = -15.943***
GenderOther		1.213 t = 14.425***		
FitzDark Fitz		1.097 t = 26.524***		
lightingDark		2.076 t = 201.974***		
GenderUnknown			1.398 t = 50.953***	
corruptiongaussian-noise	3,299,654.000 t = 2.195**	2,419,097.000 t = 1.580	1,636,633.000 t = 1.552	4,149,285.000 t = 1.644
corruptionshot-noise	3,259,061.000 t = 2.193**	1,515,211.000 t = 1.529	1,579,353.000 t = 1.548	4,907,243.000 t = 1.663*
corruptionimpulse-noise	3,002,401.000 t = 2.181**	2,342,689.000 t = 1.576	1,660,139.000 t = 1.553	3,578,501.000 t = 1.628
corruptiondefocus-blur	473,840.400 t = 1.911*	291,537.200 t = 1.352	962,996.800 t = 1.494	1,399,037.000 t = 1.527
corruptionglass-blur	475,706.900 t = 1.911*	122,767.900 t = 1.259	429,061.500 t = 1.407	1,573,367.000 t = 1.540
corruptionmotion-blur	463,205.700 t = 1.907*	236,664.500 t = 1.330	1,001,403.000 t = 1.499	1,585,644.000 t = 1.541
corruptionzoom-blur	551,933.600 t = 1.933*	19,472,611.000 t = 1.804*	3,617,701.000 t = 1.638	994,071.300 t = 1.490
corruptionsnow	2,559,910.000 t = 2.157**	2,415,036.000 t = 1.579	1,591,836.000 t = 1.549	1,836,187.000 t = 1.556
corruptionfrost	2,337,979.000 t = 2.144**	3,832,060.000 t = 1.629	1,653,085.000 t = 1.553	1,518,236.000 t = 1.536
corruptionfog	1,597,503.000 t = 2.088**	803,122.200 t = 1.461	833,146.800 t = 1.479	1,119,759.000 t = 1.503
corruptionbrightness	276,642.600 t = 1.832*	165,223.200 t = 1.291	462,113.300 t = 1.415	380,794.200 t = 1.387
corruptioncontrast	1,848,527.000 t = 2.110**	3,087,215.000 t = 1.606	1,832,109.000 t = 1.564	2,257,641.000 t = 1.579
corruptionelastic-transform	810,705.400 t = 1.989**	226,499.200 t = 1.325	569,559.100 t = 1.437	2,039,164.000 t = 1.568
corruptionpixelate	387,717.200 t = 1.881*	383,879.100 t = 1.382	887,161.300 t = 1.486	562,142.200 t = 1.429
corruptionjpeg-compression	850,378.100 t = 1.996**	216,252.800 t = 1.320	519,991.800 t = 1.428	565,216.400 t = 1.429
serviceazure	0.629 t = -128.849***	1.896 t = 145.072***	0.836 t = -35.839***	1.175 t = 41.100***
servicegep	0.689 t = -105.016***	2.138 t = 174.225***	1.037 t = 7.461***	1.699 t = 142.957***
Constant	0.00000 t = -2.261**	0.00000 t = -1.892*	0.00000 t = -1.711*	0.00000 t = -1.804*
Observations	3,401,435	4,889,232	1,868,037	5,037,951
Log Likelihood	-1,447,532.000	-1,197,724.000	-798,135.600	-1,543,860.000
Akaike Inf. Crit.	2,895,105.000	2,395,496.000	1,596,317.000	3,087,763.000

Note: *p<0.1; **p<0.05; ***p<0.01

Table 7: Full regression (odds ratio) for the Adience dataset.

	Dependent variable:			
	rCE			
	All Data (1)	Just AWS (2)	Just Azure (3)	Just GCP (4)
Age3-7	0.898 t = -16.787***	0.914 t = -8.534***	0.879 t = -10.452***	0.875 t = -11.288***
Age8-14	0.944 t = -9.076***	0.987 t = -1.225	0.899 t = -8.771***	0.922 t = -6.974***
Age15-24	1.052 t = 7.678***	1.098 t = 8.706***	1.001 t = 0.069	1.053 t = 4.276***
Age25-35	1.275 t = 41.444***	1.415 t = 36.183***	1.290 t = 22.586***	1.163 t = 13.954***
Age36-45	1.185 t = 27.943***	1.288 t = 25.457***	1.187 t = 14.653***	1.103 t = 8.777***
Age46-59	1.198 t = 23.642***	1.265 t = 18.774***	1.111 t = 7.073***	1.245 t = 15.628***
Age60+	1.313 t = 35.883***	1.383 t = 26.073***	1.319 t = 18.909***	1.299 t = 18.762***
GenderMale	1.077 t = 24.962***	1.067 t = 13.307***	1.022 t = 3.718***	1.164 t = 27.542***
corruptiongaussian-noise	3,300,849.000 t = 2.195**	5,029,800.000 t = 1.299	14,078,694.000 t = 0.840	2,745,350.000 t = 0.756
corruptionshot-noise	3,260,220.000 t = 2.193**	5,026,798.000 t = 1.299	15,464,046.000 t = 0.844	2,085,452.000 t = 0.742
corruptionimpulse-noise	3,003,342.000 t = 2.181**	4,725,483.000 t = 1.294	11,179,095.000 t = 0.828	2,925,809.000 t = 0.759
corruptiondefocus-blur	473,711.600 t = 1.911*	743,249.900 t = 1.138	809,232.700 t = 0.694	1,096,976.000 t = 0.709
corruptionglass-blur	475,577.900 t = 1.912*	743,742.200 t = 1.138	925,002.200 t = 0.701	992,259.500 t = 0.704
corruptionmotion-blur	463,078.200 t = 1.908*	631,427.400 t = 1.124	943,359.600 t = 0.702	1,151,894.000 t = 0.712
corruptionzoom-blur	551,797.100 t = 1.933*	912,873.700 t = 1.155	1,070,879.000 t = 0.708	1,042,423.000 t = 0.707
corruptionsnow	2,560,511.000 t = 2.158**	1,696,265.000 t = 1.207	2,835,738.000 t = 0.758	18,350,791.000 t = 0.853
corruptionfrost	2,338,429.000 t = 2.145**	3,484,793.000 t = 1.268	4,382,529.000 t = 0.780	5,744,206.000 t = 0.794
corruptionfog	1,597,557.000 t = 2.089**	1,075,494.000 t = 1.169	1,528,212.000 t = 0.726	10,658,256.000 t = 0.825
corruptionbrightness	276,549.500 t = 1.832*	301,646.900 t = 1.062	356,540.100 t = 0.652	1,109,229.000 t = 0.710
corruptioncontrast	1,848,683.000 t = 2.110**	1,432,724.000 t = 1.193	2,319,255.000 t = 0.748	10,424,136.000 t = 0.824
corruptionelastic-transform	810,567.800 t = 1.990**	1,062,765.000 t = 1.168	1,322,389.000 t = 0.719	2,491,531.000 t = 0.751
corruptionpixelate	387,601.000 t = 1.882*	740,494.100 t = 1.138	559,640.600 t = 0.675	680,044.900 t = 0.685
corruptionjpeg-compression	850,243.500 t = 1.997**	2,040,461.000 t = 1.223	1,296,768.000 t = 0.718	807,375.800 t = 0.694
serviceazure	0.629 t = -128.874***			
servicegcp	0.689 t = -105.037***			
Constant	0.00000 t = -2.256**	0.00000 t = -1.326	0.00000 t = -0.849	0.00000 t = -0.852
Observations	3,401,435	1,133,844	1,133,747	1,133,844
Log Likelihood	-1,447,008.000	-534,567.700	-399,381.200	-431,576.400
Akaike Inf. Crit.	2,894,069.000	1,069,183.000	798,810.400	863,200.800

Note: *p<0.1; **p<0.05; ***p<0.01

Table 8: Full regression (odds ratio) for the CCD dataset.

	Dependent variable:			
	All Data	Just AWS	Just Azure	Just GCP
	(1)	(2)	(3)	(4)
	rCE			
Age_Numeric	1.007 t = 66.760***	1.008 t = 34.779***	1.009 t = 51.660***	1.005 t = 30.681***
GenderMale	1.130 t = 35.323***	1.146 t = 18.518***	1.140 t = 23.330***	1.125 t = 20.378***
GenderOther	1.382 t = 34.253***	1.444 t = 18.407***	1.583 t = 30.584***	1.199 t = 11.325***
FitzDark Fitz	1.097 t = 26.523***	1.167 t = 20.802***	1.074 t = 12.735***	1.089 t = 14.681***
lightingDark	2.135 t = 206.954***	2.211 t = 101.589***	1.937 t = 110.748***	2.532 t = 150.449***
corruptiongaussian-noise	2,419,281.000 t = 1.580	680,001.600 t = 0.828	6,557,183.000 t = 0.966	1,126,523.000 t = 0.863
corruptionshot-noise	1,514,874.000 t = 1.530	292,706.700 t = 0.776	4,288,977.000 t = 0.939	559,769.600 t = 0.820
corruptionimpulse-noise	2,342,813.000 t = 1.577	727,125.300 t = 0.832	5,160,853.000 t = 0.951	1,737,269.000 t = 0.890
corruptiondefocus-blur	291,326.200 t = 1.353	119,493.500 t = 0.721	510,139.400 t = 0.809	259,920.600 t = 0.772
corruptionglass-blur	122,669.100 t = 1.260	49,812.830 t = 0.667	185,467.400 t = 0.746	137,736.600 t = 0.733
corruptionmotion-blur	236,487.100 t = 1.330	110,615.700 t = 0.716	343,161.100 t = 0.784	265,537.500 t = 0.773
corruptionzoom-blur	19,520,060.000 t = 1.805*	18,618,834.000 t = 1.032	12,417,638.000 t = 1.005	29,948,877.000 t = 1.066
corruptionsnow	2,415,217.000 t = 1.580	1,847,619.000 t = 0.890	1,906,318.000 t = 0.890	3,638,333.000 t = 0.936
corruptionfrost	3,833,825.000 t = 1.630	2,653,855.000 t = 0.912	3,410,599.000 t = 0.925	5,690,302.000 t = 0.963
corruptionfog	802,722.700 t = 1.462	223,413.400 t = 0.759	318,462.500 t = 0.780	2,024,326.000 t = 0.899
corruptionbrightness	165,093.700 t = 1.292	70,307.140 t = 0.688	150,148.700 t = 0.733	281,231.800 t = 0.777
corruptioncontrast	3,088,044.000 t = 1.607	1,498,911.000 t = 0.877	1,277,470.000 t = 0.865	7,968,542.000 t = 0.984
corruptionelastic-transform	226,328.300 t = 1.326	94,636.780 t = 0.706	239,821.800 t = 0.762	353,685.600 t = 0.791
corruptionpixelate	383,617.800 t = 1.382	620,480.500 t = 0.822	288,907.100 t = 0.774	259,625.100 t = 0.772
corruptionjpeg-compression	216,088.600 t = 1.321	126,196.100 t = 0.724	298,045.600 t = 0.775	232,351.600 t = 0.765
serviceazure	1.897 t = 145.130***			
servicegcp	2.140 t = 174.293***			
Constant	0.00000 t = -1.910*	0.00000 t = -1.070	0.00000 t = -1.064	0.00000 t = -1.068
Observations	4,889,232	1,629,744	1,629,744	1,629,744
Log Likelihood	-1,196,693.000	-278,407.500	-440,570.400	-417,931.900
Akaike Inf. Crit.	2,393,432.000	556,857.000	881,182.800	835,905.800

Note:

*p<0.1; **p<0.05; ***p<0.01

Table 9: Full regression (odds ratio) for the MIAP dataset.

	Dependent variable:			
	All Data	Just AWS	Just Azure	Just GCP
	(1)	(2)	(3)	(4)
AgePresentationMiddle	0.918 t = -12.127***	0.689 t = -27.939***	0.925 t = -6.035***	1.134 t = 11.134***
AgePresentationOlder	1.383 t = 57.381***	1.788 t = 61.727***	1.287 t = 24.390***	1.124 t = 11.826***
AgePresentationUnknown	0.780 t = -33.288***	0.606 t = -38.556***	0.846 t = -12.537***	0.922 t = -6.429***
GenderPresentationPredominantly Masculine	1.187 t = 29.740***	1.225 t = 20.101***	1.148 t = 13.151***	1.192 t = 18.343***
GenderPresentationUnknown	1.398 t = 50.953***	1.606 t = 42.518***	1.377 t = 26.730***	1.234 t = 18.528***
corruptiongaussian-noise	1,636,633.000 t = 1.552	1,691,049.000 t = 0.911	1,902,127.000 t = 0.903	1,348,987.000 t = 0.879
corruptionshot-noise	1,579,353.000 t = 1.548	1,641,992.000 t = 0.909	1,879,834.000 t = 0.902	1,254,371.000 t = 0.874
corruptionimpulse-noise	1,660,139.000 t = 1.553	1,745,798.000 t = 0.913	1,845,022.000 t = 0.901	1,415,442.000 t = 0.882
corruptiondefocus-blur	962,996.800 t = 1.494	1,035,071.000 t = 0.879	761,231.400 t = 0.846	1,103,270.000 t = 0.866
corruptionglass-blur	429,061.500 t = 1.407	528,138.000 t = 0.837	316,112.100 t = 0.791	444,226.500 t = 0.810
corruptionmotion-blur	1,001,403.000 t = 1.499	1,123,057.000 t = 0.885	832,488.700 t = 0.851	1,058,015.000 t = 0.864
corruptionzoom-blur	3,617,701.000 t = 1.638	4,198,146.000 t = 0.968	3,197,109.000 t = 0.935	3,581,226.000 t = 0.940
corruptionsnow	1,591,836.000 t = 1.549	1,419,027.000 t = 0.899	1,253,683.000 t = 0.877	2,162,464.000 t = 0.908
corruptionfrost	1,653,085.000 t = 1.553	1,518,481.000 t = 0.904	1,346,618.000 t = 0.881	2,140,125.000 t = 0.908
corruptionfog	833,146.800 t = 1.479	680,664.300 t = 0.853	538,483.700 t = 0.824	1,328,905.000 t = 0.878
corruptionbrightness	462,113.300 t = 1.415	443,166.200 t = 0.826	341,180.800 t = 0.795	605,453.200 t = 0.829
corruptioncontrast	1,832,109.000 t = 1.564	1,546,406.000 t = 0.905	1,287,632.000 t = 0.878	2,825,312.000 t = 0.925
corruptionelastic-transform	569,559.100 t = 1.437	702,940.300 t = 0.855	481,522.900 t = 0.817	527,140.500 t = 0.820
corruptionpixelate	887,161.300 t = 1.486	1,314,799.000 t = 0.895	615,269.900 t = 0.832	779,908.600 t = 0.845
corruptionjpeg-compression	519,991.800 t = 1.428	677,471.400 t = 0.852	489,452.800 t = 0.818	397,970.400 t = 0.803
serviceazure	0.836 t = -35.839***			
servicegcp	1.037 t = 7.461***			
Constant	0.00000 t = -1.711*	0.00000 t = -1.011	0.00000 t = -0.986	0.00000 t = -0.981
Observations	1,868,037	622,744	622,580	622,713
Log Likelihood	-798,135.600	-267,002.300	-247,142.600	-275,726.700
Akaike Inf. Crit.	1,596,317.000	534,046.600	494,327.100	551,495.400

Note:

*p<0.1; **p<0.05; ***p<0.01

Table 10: Full regression (odds ratio) for the UTKFace dataset.

	Dependent variable:			
	All Data (1)	Just AWS (2)	Just Azure (3)	Just GCP (4)
Age_Numeric	1.004 t = 52.245***	1.005 t = 35.168***	1.003 t = 18.805***	1.004 t = 36.949***
GenderMale	0.933 t = -22.982***	1.014 t = 2.448**	0.959 t = -7.393***	0.861 t = -31.589***
corruptiongaussian-noise	4,145,414.000 t = 1.643	3,734,420.000 t = 0.938	6,372,202.000 t = 0.971	2,652,515.000 t = 0.917
corruptionshot-noise	4,900,926.000 t = 1.661*	4,216,671.000 t = 0.946	7,911,105.000 t = 0.984	3,096,235.000 t = 0.927
corruptionimpulse-noise	3,576,209.000 t = 1.627	3,256,267.000 t = 0.930	5,555,750.000 t = 0.962	2,197,870.000 t = 0.906
corruptiondefocus-blur	1,400,083.000 t = 1.526	1,167,437.000 t = 0.866	820,173.100 t = 0.844	2,297,815.000 t = 0.908
corruptionglass-blur	1,574,338.000 t = 1.538	1,184,628.000 t = 0.867	1,045,880.000 t = 0.859	2,591,618.000 t = 0.916
corruptionmotion-blur	1,586,608.000 t = 1.539	1,294,999.000 t = 0.873	1,437,010.000 t = 0.878	2,063,194.000 t = 0.902
corruptionzoom-blur	995,133.000 t = 1.489	836,403.600 t = 0.846	773,236.300 t = 0.840	1,405,126.000 t = 0.878
corruptionsnow	1,836,972.000 t = 1.555	539,752.700 t = 0.818	603,558.800 t = 0.825	5,096,713.000 t = 0.958
corruptionfrost	1,519,235.000 t = 1.535	1,431,952.000 t = 0.879	894,567.500 t = 0.849	2,306,211.000 t = 0.909
corruptionfog	1,120,841.000 t = 1.502	394,172.100 t = 0.799	412,852.300 t = 0.801	2,787,153.000 t = 0.920
corruptionbrightness	381,404.400 t = 1.386	254,282.700 t = 0.772	271,459.600 t = 0.775	631,869.600 t = 0.828
corruptioncontrast	2,257,945.000 t = 1.577	966,427.300 t = 0.854	910,362.700 t = 0.850	5,668,403.000 t = 0.964
corruptionelastic-transform	2,039,749.000 t = 1.566	1,688,979.000 t = 0.889	1,170,645.000 t = 0.866	3,427,095.000 t = 0.933
corruptionpixelate	562,950.400 t = 1.427	784,093.400 t = 0.842	411,360.200 t = 0.801	508,600.900 t = 0.815
corruptionjpeg-compression	566,027.500 t = 1.428	787,528.700 t = 0.842	462,396.200 t = 0.808	463,179.500 t = 0.809
serviceazure	1.175 t = 41.060***			
servicegcp	1.698 t = 142.849***			
Constant	0.00000 t = -1.822*	0.00000 t = -1.038	0.00000 t = -1.030	0.00000 t = -1.031
Observations	5,037,951	1,679,524	1,679,055	1,679,372
Log Likelihood	-1,546,513.000	-441,524.100	-443,349.100	-609,017.200
Akaike Inf. Crit.	3,093,066.000	883,084.300	886,734.300	1,218,070.000

Note: *p<0.1; **p<0.05; ***p<0.01

Table 11: Interaction (odds ratio) of Age and Gender for the Adience dataset.

	Dependent variable:								
	Interaction (1)	Just 0-2 (2)	Just 3-7 (3)	Just 8-14 (4)	rCE Just 15-24 (5)	Just 25-35 (6)	Just 36-45 (7)	Just 46-59 (8)	Just 60+ (9)
age_group3-7	0.899 t = -12.543***								
age_group8-14	0.990 t = -1.224								
age_group15-24	0.992 t = -0.918								
age_group25-35	1.219 t = 24.812***								
age_group36-45	1.128 t = 14.205***								
age_group46-59	1.106 t = 9.502***								
age_group60+	1.139 t = 12.282***								
genderMale	1.027 t = 2.811***	1.027 t = 2.811***	1.040 t = 4.914***	0.915 t = -11.513***	1.153 t = 17.221***	1.069 t = 11.078***	1.091 t = 12.776***	1.157 t = 13.046***	1.271 t = 21.839***
age_group3-7:genderMale	1.012 t = 1.011								
age_group8-14:genderMale	0.892 t = -9.458***								
age_group15-24:genderMale	1.123 t = 9.270***								
age_group25-35:genderMale	1.041 t = 3.592***								
age_group36-45:genderMale	1.062 t = 5.206***								
age_group46-59:genderMale	1.126 t = 8.166***								
age_group60+:genderMale	1.238 t = 14.761***								
Constant	0.208 t = -232.438***	0.208 t = -232.438***	0.187 t = -321.492***	0.206 t = -327.944***	0.207 t = -288.280***	0.254 t = -319.931***	0.235 t = -279.896***	0.230 t = -179.338***	0.237 t = -175.725***
Observations	3,356,678	315,000	485,318	514,308	402,522	674,989	560,233	202,938	201,370
Log Likelihood	-1,609,029.000	-145,767.100	-213,324.700	-231,135.300	-189,651.600	-345,118.800	-278,814.300	-101,257.600	-103,959.300
Akaike Inf. Crit.	3,218,089.000	291,538.200	426,653.500	462,274.500	379,307.300	690,241.600	557,632.500	202,519.300	207,922.600

Note:

*p<0.1; **p<0.05; ***p<0.01

Table 12: Interaction (odds ratio) of Lighting and Skin Type for the CCD dataset.

	Dependent variable:		
	Interaction (1)	rCE Just dark Lighting (2)	Just light Lighting (3)
lightingDark	1.804 t = 115.964***		
FitzDark Fitz	1.083 t = 20.524***	1.027 t = 5.111***	1.083 t = 20.524***
lightingDark:FitzDark Fitz	0.948 t = -8.234***		
Constant	0.090 t = -868.977***	0.162 t = -426.198***	0.090 t = -868.977***
Observations	4,824,900	1,422,900	3,402,000
Log Likelihood	-1,575,840.000	-581,078.700	-994,761.100
Akaike Inf. Crit.	3,151,688.000	1,162,161.000	1,989,526.000

Note:

*p<0.1; **p<0.05; ***p<0.01

Table 13: Interaction (odds ratio) of Lighting and Age for the CCD dataset.

	Dependent variable:		
	Interaction (1)	rCE Just dark Lighting (2)	Just light Lighting (3)
lightingDark	1.887 t = 148.921***		
Age45-64	1.150 t = 32.852***	1.078 t = 13.765***	1.150 t = 32.852***
Age65+	1.284 t = 44.789***	1.178 t = 17.206***	1.284 t = 44.789***
lightingDark:Age45-64	0.937 t = -9.414***		
lightingDark:Age65+	0.918 t = -7.783***		
Constant	0.085 t = -807.913***	0.160 t = -614.951***	0.085 t = -807.913***
Observations	4,824,900	1,422,900	3,402,000
Log Likelihood	-1,574,722.000	-580,886.600	-993,835.600
Akaike Inf. Crit.	3,149,456.000	1,161,779.000	1,987,677.000

Note:

*p<0.1; **p<0.05; ***p<0.01

Table 14: Interaction (odds ratio) of Lighting and Age (as a numeric variable) for the CCD dataset.

	<i>Dependent variable:</i>
	rCE
lightingDark	1.952 t = 80.718***
Age_Numeric	1.005 t = 48.335***
lightingDark:Age_Numeric	0.998 t = -9.639***
Constant	0.075 t = -504.962***
Observations	4,824,900
Log Likelihood	-1,574,663.000
Akaike Inf. Crit.	3,149,334.000
<i>Note:</i>	*p<0.1; **p<0.05; ***p<0.01

Table 15: Interaction (odds ratio) of Lighting and Gender for the CCD dataset.

	Dependent variable:		
	Interaction (1)	rCE Just dark Lighting (2)	Just light Lighting (3)
lightingDark	1.819 t = 135.888***		
GenderMale	1.126 t = 29.668***	1.060 t = 11.895***	1.126 t = 29.668***
GenderOther	1.053 t = 5.870***	1.145 t = 8.063***	1.053 t = 5.870***
lightingDark:GenderMale	0.941 t = -9.608***		
lightingDark:GenderOther	1.088 t = 4.447***		
Constant	0.088 t = -843.455***	0.161 t = -548.811***	0.088 t = -843.455***
Observations	4,824,900	1,422,900	3,402,000
Log Likelihood	-1,575,531.000	-581,000.400	-994,530.700
Akaike Inf. Crit.	3,151,074.000	1,162,007.000	1,989,067.000

Note:

*p<0.1; **p<0.05; ***p<0.01

Table 16: Interaction (odds ratio) of Age and Gender for the CCD dataset.

	Dependent variable:			
	Interaction	rCE		
	(1)	Just 19-45 (2)	Just 45-64 (3)	Just 65+ (4)
Age45-64	0.967 t = -7.088***			
Age65+	1.005 t = 0.682			
GenderMale	1.040 t = 9.019***	1.040 t = 9.019***	1.107 t = 20.113***	1.138 t = 15.471***
GenderOther	0.907 t = -10.490***	0.907 t = -10.490***	0.922 t = -5.404***	3.074 t = 28.170***
Age45-64:GenderMale	1.064 t = 9.266***			
Age65+:GenderMale	1.094 t = 9.519***			
Age45-64:GenderOther	1.016 t = 0.929			
Age65+:GenderOther	3.388 t = 29.814***			
Constant	0.112 t = -708.886***	0.112 t = -708.886***	0.108 t = -625.073***	0.112 t = -373.867***
Observations	4,824,900	2,435,175	1,783,125	606,600
Log Likelihood	-1,591,531.000	-799,698.200	-585,369.000	-206,464.100
Akaike Inf. Crit.	3,183,080.000	1,599,402.000	1,170,744.000	412,934.200

Note:

*p<0.1; **p<0.05; ***p<0.01

Table 17: Interaction (odds ratio) of Age and Skin Type for the CCD dataset.

	Dependent variable:			
	Interaction	rCE		
	(1)	Just 19-45	Just 45-64	Just 65+
	(1)	(2)	(3)	(4)
Age45-64	1.133 t = 24.306***			
Age65+	1.229 t = 31.779***			
FitzDark Fitz	1.300 t = 59.191***	1.300 t = 59.191***	1.071 t = 13.846***	1.047 t = 5.506***
Age45-64:FitzDark Fitz	0.824 t = -28.986***			
Age65+:FitzDark Fitz	0.806 t = -22.705***			
Constant	0.096 t = -659.001***	0.096 t = -659.001***	0.109 t = -600.022***	0.118 t = -394.225***
Observations	4,824,900	2,435,175	1,783,125	606,600
Log Likelihood	-1,590,420.000	-798,039.400	-585,515.600	-206,865.000
Akaike Inf. Crit.	3,180,852.000	1,596,083.000	1,171,035.000	413,734.000

Note:

*p<0.1; **p<0.05; ***p<0.01

Table 18: Interaction (odds ratio) of Age, Skin Type, and Gender for the CCD dataset.

	<i>Dependent variable:</i>
	rCE
Age45-64	1.072 t = 9.532***
Age65+	1.112 t = 11.247***
FitzDark Fitz	1.224 t = 31.723***
GenderMale	0.951 t = -6.830***
GenderOther	0.914 t = -5.774***
Age45-64:FitzDark Fitz	0.845 t = -17.524***
Age65+:FitzDark Fitz	0.854 t = -11.784***
Age45-64:GenderMale	1.116 t = 10.457***
Age65+:GenderMale	1.206 t = 14.308***
Age45-64:GenderOther	0.940 t = -1.777*
Age65+:GenderOther	3.348 t = 28.779***
FitzDark Fitz:GenderMale	1.141 t = 14.414***
FitzDark Fitz:GenderOther	0.980 t = -1.046
Age45-64:FitzDark Fitz:GenderMale	0.951 t = -3.665***
Age65+:FitzDark Fitz:GenderMale	0.868 t = -7.318***
Age45-64:FitzDark Fitz:GenderOther	1.108 t = 2.521**
Age65+:FitzDark Fitz:GenderOther	
Constant	0.099 t = -459.672***
Observations	4,824,900
Log Likelihood	-1,589,472.000
Akaike Inf. Crit.	3,178,977.000

Note: *p<0.1; **p<0.05; ***p<0.01

Table 19: Interaction (odds ratio) of Age (as a numeric variable) and Gender for the CCD dataset.

	<i>Dependent variable:</i>
	rCE
Age_Numeric	1.000 t = 0.787
GenderMale	0.954 t = -5.376***
GenderOther	0.879 t = -12.422***
Age_Numeric:GenderMale	1.003 t = 14.749***
Age_Numeric:GenderOther	1.008 t = 19.447***
Constant	0.110 t = -356.931***
Observations	4,824,900
Log Likelihood	-1,591,602.000
Akaike Inf. Crit.	3,183,215.000
<i>Note:</i>	*p<0.1; **p<0.05; ***p<0.01

Table 20: Interaction (odds ratio) of Age (as a numeric variable) and Skin Type for the CCD dataset.

	<i>Dependent variable:</i>
	rCE
Age_Numeric	1.005 t = 35.652***
FitzDark Fitz	1.385 t = 40.931***
Age_Numeric:FitzDark Fitz	0.996 t = -22.385***
Constant	0.085 t = -398.455***
Observations	4,824,900
Log Likelihood	-1,590,484.000
Akaike Inf. Crit.	3,180,977.000
<i>Note:</i>	*p<0.1; **p<0.05; ***p<0.01

Table 21: Interaction (odds ratio) of Gender and Skin Type for the CCD dataset.

	Dependent variable:			
	Interaction (1)	Just Male (2)	Just Female (3)	Just Other (4)
GenderMale	1.033 t = 6.883***			
GenderOther	0.875 t = -9.746***			
FitzDark Fitz	1.123 t = 26.434***	1.213 t = 43.854***	1.123 t = 26.431***	1.228 t = 12.914***
GenderMale:FitzDark Fitz	1.080 t = 12.364***			
GenderOther:FitzDark Fitz	1.094 t = 5.436***			
Constant	0.103 t = -683.043***	0.107 t = -672.156***	0.103 t = -682.936***	0.090 t = -181.136***
Observations	4,824,900	2,232,225	2,375,325	217,350
Log Likelihood	-1,590,636.000	-754,509.000	-768,396.800	-67,730.120
Akaike Inf. Crit.	3,181,284.000	1,509,022.000	1,536,798.000	135,464.200

Note:

*p<0.1; **p<0.05; ***p<0.01

Table 22: Interaction (odds ratio) of Age and Gender for the MIAP dataset.

	Dependent variable:						
	Interaction (1)	Just Young (2)	Just Middle (3)	tCE Just Old (4)	Just Feminine (5)	Just Masculine (6)	Just Unknown (7)
AgePresentationMiddle	0.675 t = -19.644***				0.675 t = -19.644***	0.809 t = -19.982***	0.957 t = -0.932
AgePresentationOlder	1.270 t = 15.832***				1.270 t = 15.832***	1.280 t = 20.790***	1.852 t = 58.289***
AgePresentationUnknown	0.856 t = -13.842***						0.856 t = -13.842***
GenderPresentationPredominantly Masculine	1.163 t = 17.934***	1.163 t = 17.934***	1.395 t = 15.833***	1.172 t = 9.211***			
GenderPresentationUnknown	1.190 t = 15.478***	1.190 t = 15.478***	1.688 t = 10.466***	1.735 t = 37.711***			
AgePresentationMiddle:GenderPresentationPredominantly Masculine	1.199 t = 8.019***						
AgePresentationOlder:GenderPresentationPredominantly Masculine	1.008 t = 0.394						
AgePresentationUnknown:GenderPresentationPredominantly Masculine							
AgePresentationMiddle:GenderPresentationUnknown	1.418 t = 6.820***						
AgePresentationOlder:GenderPresentationUnknown	1.458 t = 20.468***						
AgePresentationUnknown:GenderPresentationUnknown							
Constant	0.159 t = -299.959***	0.159 t = -299.959***	0.108 t = -116.917***	0.202 t = -115.744***	0.159 t = -299.959***	0.185 t = -290.356***	0.190 t = -176.549***
Observations	1,228,938	534,150	147,075	322,713	293,850	397,415	537,673
Log Likelihood	-545,873.700	-224,575.000	-54,955.920	-175,345.900	-117,066.700	-170,469.000	-258,338.000
Akaike Inf. Crit.	1,091,767.000	449,155.900	109,917.800	350,697.900	234,139.400	340,944.100	516,684.000

Note: *p<0.1; **p<0.05; ***p<0.01

Table 23: Interaction (odds ratio) of Age and Gender for the UTKFace dataset.

	<i>Dependent variable:</i>				
	Interaction (1)	Just 0-18 (2)	<i>rCE</i> Just 19-45 (3)	Just 45-64 (4)	Just 65+ (5)
Age19-45	0.855 t = -22.893***				
Age45-64	0.964 t = -3.723***				
Age65+	1.287 t = 25.011***				
genderMale	0.945 t = -6.807***	0.945 t = -6.807***	1.009 t = 1.710*	1.036 t = 3.620***	0.914 t = -7.823***
Age19-45:genderMale	1.069 t = 6.625***				
Age45-64:genderMale	1.096 t = 7.198***				
Age65+:genderMale	0.968 t = -2.298**				
Constant	0.105 t = -395.638***	0.105 t = -395.638***	0.090 t = -631.394***	0.101 t = -282.362***	0.135 t = -239.992***
Observations	3,314,387	678,662	1,728,150	606,600	300,975
Log Likelihood	-1,000,139.000	-209,933.600	-493,906.800	-189,325.500	-106,973.500
Akaike Inf. Crit.	2,000,295.000	419,871.200	987,817.600	378,654.900	213,951.000

Note:

*p<0.1; **p<0.05; ***p<0.01

Table 24: Interaction (odds ratio) of Age and Ethnicity for the UTKFace dataset.

	Dependent variable:				
	Interaction (1)	Just 0-18 (2)	<i>rCE</i> Just 19-45 (3)	Just 45-64 (4)	Just 65+ (5)
Age19-45	0.780 t = -15.801***				
Age45-64	0.781 t = -7.867***				
Age65+	1.800 t = 8.801***				
ethnicityWhite	1.215 t = 14.166***	1.215 t = 14.166***	1.191 t = 15.760***	1.412 t = 11.706***	0.719 t = -5.010***
ethnicityBlack	0.882 t = -5.821***	0.882 t = -5.821***	1.328 t = 25.779***	1.357 t = 9.849***	0.731 t = -4.640***
ethnicityAsian	1.004 t = 0.283	1.004 t = 0.283	1.084 t = 6.786***	1.080 t = 2.177**	0.683 t = -5.619***
ethnicityIndian	0.607 t = -26.663***	0.607 t = -26.663***	1.062 t = 5.245***	1.221 t = 6.512***	0.741 t = -4.335***
Age19-45:ethnicityWhite	0.980 t = -1.119				
Age45-64:ethnicityWhite	1.162 t = 4.618***				
Age65+:ethnicityWhite	0.591 t = -7.795***				
Age19-45:ethnicityBlack	1.505 t = 16.911***				
Age45-64:ethnicityBlack	1.539 t = 11.411***				
Age65+:ethnicityBlack	0.828 t = -2.656***				
Age19-45:ethnicityAsian	1.079 t = 3.996***				
Age45-64:ethnicityAsian	1.076 t = 1.896*				
Age65+:ethnicityAsian	0.680 t = -5.548***				
Age19-45:ethnicityIndian	1.751 t = 25.455***				
Age45-64:ethnicityIndian	2.012 t = 19.454***				
Age65+:ethnicityIndian	1.221 t = 2.785***				
Constant	0.100 t = -186.123***	0.100 t = -186.123***	0.078 t = -262.518***	0.078 t = -88.297***	0.180 t = -26.173***
Observations	3,314,537	678,662	1,728,150	606,750	300,975
Log Likelihood	-998,180.900	-208,711.700	-493,285.800	-189,196.900	-106,986.500
Akaike Inf. Crit.	1,996,402.000	417,433.400	986,581.500	378,403.700	213,983.100

Note:

*p<0.1; **p<0.05; ***p<0.01

Table 25: Interaction (odds ratio) of Gender and Ethnicity for the UTKFace dataset.

	Dependent variable:		
	Interaction (1)	rCE Just Male (2)	Just Female (3)
genderMale	0.822 t = -13.125***		
ethnicityWhite	1.198 t = 17.206***	1.420 t = 28.782***	1.198 t = 17.206***
ethnicityBlack	1.074 t = 6.190***	1.424 t = 27.375***	1.074 t = 6.190***
ethnicityAsian	0.957 t = -3.732***	1.251 t = 16.519***	0.957 t = -3.732***
ethnicityIndian	0.908 t = -8.045***	1.084 t = 6.121***	0.908 t = -8.045***
genderMale:ethnicityWhite	1.186 t = 10.601***		
genderMale:ethnicityBlack	1.326 t = 16.291***		
genderMale:ethnicityAsian	1.306 t = 14.934***		
genderMale:ethnicityIndian	1.194 t = 9.945***		
Constant	0.093 t = -249.112***	0.076 t = -224.112***	0.093 t = -249.112***
Observations	3,314,387	1,729,045	1,585,342
Log Likelihood	-1,000,032.000	-522,244.200	-477,787.900
Akaike Inf. Crit.	2,000,084.000	1,044,498.000	955,585.700

Note:

*p<0.1; **p<0.05; ***p<0.01

Table 26: Gender estimation (odds ratio) for the all datasets with unified demographic variables.

	Dependent variable:			
	Adience (1)	pred_gender_iswrong CCD (2)	MIAP (3)	UTKFace (4)
AgeMiddle	0.583 t = -96.002***			0.179 t = -350.850***
AgeOlder	0.880 t = -11.434***	1.078 t = 11.006***	0.696 t = -36.178***	0.301 t = -150.403***
AgeUnknown			8.443 t = 174.537***	
GenderMale	2.071 t = 134.989***	1.116 t = 23.976***	1.121 t = 14.530***	2.818 t = 220.342***
FitzDark Fitz		1.079 t = 16.184***		
lightingDark		1.354 t = 61.186***		
corruptiongaussian-noise	145.682 t = 47.496***	7.920 t = 62.209***	2.790 t = 25.488***	6.713 t = 68.826***
corruptionshot-noise	147.362 t = 47.605***	6.795 t = 57.514***	2.847 t = 25.995***	7.786 t = 74.285***
corruptionimpulse-noise	147.129 t = 47.590***	7.899 t = 62.126***	2.914 t = 26.580***	6.284 t = 66.400***
corruptiondefocus-blur	4.395 t = 13.825***	1.293 t = 7.346***	1.840 t = 15.043***	3.100 t = 40.406***
corruptionglass-blur	6.548 t = 17.675***	1.027 t = 0.747	1.218 t = 4.822***	3.110 t = 40.533***
corruptionmotion-blur	6.194 t = 17.137***	1.236 t = 6.038***	1.965 t = 16.689***	2.775 t = 36.359***
corruptionzoom-blur	2.716 t = 9.210***	29.180 t = 101.740***	6.835 t = 47.732***	2.036 t = 25.103***
corruptionsnow	70.237 t = 40.521***	7.491 t = 60.502***	2.537 t = 23.100***	1.982 t = 24.130***
corruptionfrost	111.544 t = 44.946***	7.384 t = 60.061***	2.639 t = 24.091***	2.997 t = 39.179***
corruptionfog	53.631 t = 37.936***	1.856 t = 17.983***	1.576 t = 11.191***	1.773 t = 20.119***
corruptionbrightness	5.930 t = 16.717***	1.177 t = 4.627***	1.264 t = 5.717***	1.179 t = 5.693***
corruptioncontrast	52.358 t = 37.706***	4.523 t = 45.033***	2.835 t = 25.890***	2.865 t = 37.533***
corruptionelastic-transform	17.303 t = 27.059***	1.122 t = 3.269***	1.347 t = 7.295***	2.549 t = 33.262***
corruptionpixelate	1.519 t = 3.753***	1.815 t = 17.311***	2.045 t = 17.690***	1.459 t = 13.164***
corruptionjpeg-compression	46.467 t = 36.561***	1.440 t = 10.471***	1.421 t = 8.621***	1.637 t = 17.270***
Constant	0.005 t = -50.466***	0.041 t = -97.088***	0.209 t = -41.232***	0.126 t = -76.778***
Observations	1,133,844	1,556,328	350,284	1,679,524
Log Likelihood	-436,380.100	-617,369.600	-204,156.500	-664,481.800
Akaike Inf. Crit.	872,798.300	1,234,779.000	408,350.900	1,329,002.000

Note: *p<0.1; **p<0.05; ***p<0.01

Table 27: Gender prediction (odds ratio) for the Adience dataset.

	<i>Dependent variable:</i> pred_gender_iswrong
Age3-7	1.092 t = 8.348***
Age8-14	0.972 t = -2.706***
Age15-24	0.679 t = -34.018***
Age25-35	0.511 t = -64.562***
Age36-45	0.557 t = -54.886***
Age46-59	0.623 t = -34.310***
Age60+	0.822 t = -14.670***
GenderMale	2.065 t = 133.934***
corruptiongaussian-noise	147.073 t = 47.582***
corruptionshot-noise	148.776 t = 47.692***
corruptionimpulse-noise	148.540 t = 47.677***
corruptiondefocus-blur	4.397 t = 13.829***
corruptionglass-blur	6.554 t = 17.681***
corruptionmotion-blur	6.199 t = 17.143***
corruptionzoom-blur	2.717 t = 9.212***
corruptionsnow	70.692 t = 40.579***
corruptionfrost	112.481 t = 45.022***
corruptionfog	53.923 t = 37.985***
corruptionbrightness	5.935 t = 16.723***
corruptioncontrast	52.638 t = 37.753***
corruptionelastic-transform	17.342 t = 27.078***
corruptionpixelate	1.519 t = 3.754***
corruptionjpeg-compression	46.696 t = 36.604***
Constant	0.005 t = -49.725***
Observations	1,133,844
Log Likelihood	-435,061.800
Akaike Inf. Crit.	870,171.600

Note: *p<0.1; **p<0.05; ***p<0.01

Table 28: Gender estimation (odds ratio) for the CCD dataset.

	Dependent variable:	
	pred_gender_iswrong	
Age_Numeric	1.000	t = -3.126***
GenderMale	1.114	t = 23.716***
FitzDark Fitz	1.073	t = 14.978***
lightingDark	1.342	t = 58.560***
corruptiongaussian-noise	7.919	t = 62.206***
corruptionshot-noise	6.794	t = 57.512***
corruptionimpulse-noise	7.898	t = 62.123***
corruptiondefocus-blur	1.293	t = 7.345***
corruptionglass-blur	1.027	t = 0.747
corruptionmotion-blur	1.236	t = 6.038***
corruptionzoom-blur	29.170	t = 101.732***
corruptionsnow	7.490	t = 60.500***
corruptionfrost	7.383	t = 60.058***
corruptionfog	1.856	t = 17.983***
corruptionbrightness	1.177	t = 4.627***
corruptioncontrast	4.522	t = 45.031***
corruptionelastic-transform	1.122	t = 3.269***
corruptionpixelate	1.815	t = 17.311***
corruptionjpeg-compression	1.440	t = 10.471***
Constant	0.043	t = -94.100***
Observations	1,556,328	
Log Likelihood	-617,424.800	
Akaike Inf. Crit.	1,234,890.000	

Note: *p<0.1; **p<0.05; ***p<0.01

Table 29: Gender estimation (odds ratio) for the MIAP dataset.

	<i>Dependent variable:</i> pred_gender_iswrong
AgePresentationOlder	0.696 t = -36.178***
AgePresentationUnknown	8.443 t = 174.537***
GenderPresentationPredominantly Masculine	1.121 t = 14.530***
corruptiongaussian-noise	2.790 t = 25.488***
corruptionshot-noise	2.847 t = 25.995***
corruptionimpulse-noise	2.914 t = 26.580***
corruptiondefocus-blur	1.840 t = 15.043***
corruptionglass-blur	1.218 t = 4.822***
corruptionmotion-blur	1.965 t = 16.689***
corruptionzoom-blur	6.835 t = 47.732***
corruptionsnow	2.537 t = 23.100***
corruptionfrost	2.639 t = 24.091***
corruptionfog	1.576 t = 11.191***
corruptionbrightness	1.264 t = 5.717***
corruptioncontrast	2.835 t = 25.890***
corruptionelastic-transform	1.347 t = 7.295***
corruptionpixelate	2.045 t = 17.690***
corruptionjpeg-compression	1.421 t = 8.621***
Constant	0.209 t = -41.232***
Observations	350,284
Log Likelihood	-204,156.500
Akaike Inf. Crit.	408,350.900

Note: *p<0.1; **p<0.05; ***p<0.01

Table 30: Gender estimation (odds ratio) for the UTKFace dataset.

	<i>Dependent variable:</i>
	pred_gender_iswrong
Age_Numeric	0.974 t = -225.620***
GenderMale	2.804 t = 225.578***
corruptiongaussian-noise	6.064 t = 66.509***
corruptionshot-noise	6.976 t = 71.769***
corruptionimpulse-noise	5.699 t = 64.174***
corruptiondefocus-blur	2.931 t = 39.199***
corruptionglass-blur	2.940 t = 39.321***
corruptionmotion-blur	2.640 t = 35.305***
corruptionzoom-blur	1.971 t = 24.444***
corruptionsnow	1.921 t = 23.503***
corruptionfrost	2.839 t = 38.018***
corruptionfog	1.728 t = 19.618***
corruptionbrightness	1.172 t = 5.574***
corruptioncontrast	2.722 t = 36.434***
corruptionelastic-transform	2.437 t = 32.321***
corruptionpixelate	1.436 t = 12.862***
corruptionjpeg-compression	1.603 t = 16.853***
Constant	0.091 t = -90.381***
Observations	1,679,524
Log Likelihood	-698,055.600
Akaike Inf. Crit.	1,396,147.000

Note: *p<0.1; **p<0.05; ***p<0.01

Table 31: Age estimation for the CCD dataset.

	<i>Dependent variable:</i>
	diff_pred_age
Age_Numeric	0.634*** (0.001)
GenderMale	-2.866*** (0.017)
GenderOther	-11.029*** (0.044)
FitzDark Fitz	1.869*** (0.016)
lightingDark	0.697*** (0.019)
corruptiongaussian-noise	6.525*** (0.075)
corruptionshot-noise	4.967*** (0.075)
corruptionimpulse-noise	6.646*** (0.075)
corruptiondefocus-blur	0.528*** (0.075)
corruptionglass-blur	0.361*** (0.075)
corruptionmotion-blur	1.569*** (0.075)
corruptionzoom-blur	4.706*** (0.080)
corruptionsnow	2.723*** (0.075)
corruptionfrost	0.824*** (0.076)
corruptionfog	3.288*** (0.075)
corruptionbrightness	0.863*** (0.075)
corruptioncontrast	4.763*** (0.075)
corruptionelastic-transform	-0.482*** (0.075)
corruptionpixelate	0.622*** (0.075)
corruptionjpeg-compression	-0.942*** (0.075)
Constant	-20.136*** (0.073)
Observations	1,538,072
Log Likelihood	-5,723,810.000
Akaike Inf. Crit.	11,447,661.000

Note: *p<0.1; **p<0.05; ***p<0.01

Table 32: Age estimation for the UTKFace dataset.

	<i>Dependent variable:</i>
	pred_gender_iswrong
Age_Numeric	−0.004*** (0.00001)
GenderMale	0.135*** (0.001)
corruptiongaussian-noise	0.091*** (0.002)
corruptionshot-noise	0.107*** (0.002)
corruptionimpulse-noise	0.113*** (0.002)
corruptiondefocus-blur	0.090*** (0.002)
corruptionglass-blur	0.071*** (0.002)
corruptionmotion-blur	0.052*** (0.002)
corruptionzoom-blur	0.041*** (0.002)
corruptionsnow	0.051*** (0.002)
corruptionfrost	0.053*** (0.002)
corruptionfog	0.042*** (0.002)
corruptionbrightness	0.011*** (0.002)
corruptioncontrast	0.067*** (0.002)
corruptionelastic-transform	0.031*** (0.002)
corruptionpixelate	0.009*** (0.002)
corruptionjpeg-compression	0.017*** (0.002)
Constant	0.121*** (0.002)
Observations	1,590,377
Log Likelihood	−438,654.600
Akaike Inf. Crit.	877,345.200

Note: *p<0.1; **p<0.05; ***p<0.01